TEI of Crete
Technological Educational Institute of Crete

M.Sc. in Energy Systems

Fraunhofer
IWES

Division Systems Engineering and Distribution Grids
Department Converter Technology

Post Graduate Thesis:

« Comparative Study and experimental Verification of current sensing Technologies for high frequency inductive power transfer Systems»

The Graduate Student:

Konstantinos Salonikios

Supervisor:
Georgios Lempidis, Researcher at Fraunhofer IWES

Kassel, March 2017

ΜΕΤΑΠΤΥΧΙΑΚΗ ΕΡΓΑΣΙΑ:	**«Μελέτη σύγκρισης και πειραματική επαλήθευση, τεχνολογιών ανίχνευσης ρεύματος για συστήματα μεταφοράς ενέργειας υψηλής συχνότητας»**
ΦΟΙΤΗΤΗΣ:	**Κωνσταντίνος Σαλονικιός**
ΕΠΙΒΛΕΠΩΝ:	**Γεώργιος Λεμπίδης, Ερευνητής στο Fraunhofer IWES, Kassel**
ΑΚΑΔΗΜΑΪΚΟ ΕΤΟΣ:	**2016-17**

Σύνοψη

Η διπλωματική εργασία αποσκοπεί στην κατανοήση των τεχνολογιών μέτρησεις ρεύματος, που βρίσκουν εφαρμογή σε συστήματα επαγωγική μεταφοράς. Πραγματοποιείται μελέτη των τεχνολογιών αυτών καθώς και των στοιχείων αυτών που τα συνοδευουν. Ακόμη, πραγματοποιείται η κατασκευή τους σε εργαστηριακό περιβάλλον, έτσι ώστε να παρέχεται μια τεκμιριωμένη επιστημονική λύση, λαμβάνοντας υπόψην σημαντικούς παράγοντες για την ορθή λειτουργία των συστημάτων αυτών.

Περίληψη

Στην παρουσα εργασία διεξαγεται μία έρευνα στις τεχνολογίες αισθητήρων ρεύματος, που υπάρχουν ή και που μπορούν να σχεδιαστούν στο εργαστήριο για ειδικές εφαρμογές, όπως στην περίπτωση μας της επαγώγικής μεταφοράς ενέργειας. Πραγματοποιείται μελέτη και σύγκριση στις τεχνολογίες των μετατροπέων απο αναλογικό σε ψηφιακό σήμα (ADC) και των τεχνολογιών απομόνωσης (galvanic isolation) που βρίσκουν εφαρμογή σε ένα εκτυπωμένο κύκλωμα πλακέτας (PCB).

Παρουσιάζονται συνοπτικοί πίνακες με τα χαρακτηριστηκά των τεχνολογιών αυτών, που βρίσκονται σε ένα φύλλο δεδομένων (data sheet) και λαμβάνονται υπόψην κατα την επιλογή των στοιχείων. Πραγματοποιείται μία προσέγγιση με το συνδυασμό αυτών των τεχνολογιών ώστε να μπορέσουμε να πάρουμε το μεγιστο δυνατό αποτέλεσμα απο την συνδυαστική λειτουργία τους.

Πραγματοποιείται μελέτη για Rogowski πηνία, απο την οποία προκύπτει η σχεδίαση και η κατασκευή δύο Rogowski πηνίων, του Planar Rogowski Coil (PRC) και του Compine Rogowski Coil (CRC). Όπου και παρουσιάζονται αναλυτικά οι εξισώσεις, τα κυκλώματα και ο τρόπος κατασκευής τους.

Ακόμη σχεδιάζονται τα κυκλώματα ενός αισθητήρα Magnetoresistive (CMS 3015), ενός Shunt Resistor (FC4L) αισθητήρα ρεύματος και ενός Fluxgate (CaSR-15NP) αισθητήρα ρευματος, όπου παρουσιάζονται τα κυκλώματα τους πάνω σε μια πλακέτα (PCB). Για την σχεδίαση των κυκλωμάτων χρησιμοποιήθηκε το λογισμικό Altium Designer.

POST-GRADUATE THESIS:	**«*Comparative Study and experimental Verification of current sensing Technologies for high frequency inductive power transfer Systems*»**
STUDENT:	**Konstantinos Salonikios**
SUPERVISOR:	**Georgios Lempidis, Researcher at Fraunhofer IWES in Kassel**
ACADEMIC YEAR:	**2016-17**

Abstract

The thesis aims to present and explain the current measuring technologies, which find application in inductive transfer systems. A study of these technologies was carried out, as well the factors that affect them. Also, their construction took place in the laboratory, so as to provide a scientific solution, taking into consideration important factors for the proper operation of these systems.

Summary

In the work presented, a research on current sensor technologies that already exist or that can be designed in the laboratory for specific applications, was conducted. We carried out a research and a comparison of the technologies of converters from analog to digital (ADC) and isolation technologies (galvanic isolation) that can be applied to a printed circuit board (PCB).

A summary table with the features of these technologies was presented, which are in a data sheet and taken into consideration during the selection of the elements. We approached the experiment by combining these technologies so that we can get the maximum results from their combined operation

There is a study on the Rogowski coils, which follows the design and construction of two Rogowski coils, the Planar Rogowski Coil (PRC) and Combine Rogowski Coil (CRC). The equations, the circuits and the method of construction are presented.

In addition, the circuits of a Magnetoresistive sensor (CMS 3015), a Shunt Resistor (FC4L) current sensor and a Fluxgate (CaSR-15NP) current sensor were designed, whose circuits are presented on a printed circuit board (PCB). For the design of the circuit, the Altium Designer Software was used.

«Στον δρόμο της Αρετής οι θεοί έβαλαν από την αρχή του, τον ιδρώτα. Δρόμος στενός και ανηφορικός και δύσβατος φέρει σ'αυτήν σαν ξεκινάς. Όταν όμως αξιωθής και φθάσεις στο άκρο, εύκολος είναι έπειτα, αν κι έχη πάντα κόπους.»

Ησίοδος, 7ος αιών π.Χ.

Acknowledgements

This work would not have been completed without the help of many people to whom I would like to express my gratitude.

I would like to sincerely thank my supervisor Georgio Lempidi, researcher in Fraunhofer IWES, for supporting me during the entire duration of my presence at the Institute.

Another person from the Fraunhofer IWES, I would like to personally thank is Dr. Marco Jung, who showed trust in me. Also, I would like to thank is Dr. Jörg Kirchhoff for his help in laboratory part and the help that he provided me with measurements in his laboratory.

Finally, I would like to thank my parents, who have always been by my side, during good and bad times.

Thanks

Ευχαριστίες

Η εργασία αυτή δεν θα μπορούσε να πραγματοποιηθεί χωρίς τη βοήθεια και την υποστήριξη αρκετών ανθρώπων, στους οποίους θα ήθελα να εκφράσω την ευγνωμοσύνη μου.

Θα ήθελα να ευχαριστήσω προσωπικά τον επιβλέποντα μου ερευνητή Γεώργιο Λεμπίδη στο Fraunhofer IWES, για την στήριξη του καθ' όλη διάρκεια της παρουσίας μου στο Ινστιτούτο και εκτός αυτού.

Ένα άλλο πρόσωπο από το Fraunhofer IWES που θα ήθελα να ευχαριστήσω προσωπικά είναι ο Δρ. Marco Jung, που έδειξε την εμπιστοσύνη του στο πρόσωπο μου. Θα ήθελα επίσης να ευχριστήσω τον Δρ Jörg Kirchhoff για την βοήθεια του στο εργαστηριακό μέρος της εργασίας και την βοήθεια που παρείχε στις μετρήσεις στον χωρο του εργαστηρίου του

Τέλος, θέλω να δώσω ένα μεγάλο ευχαριστήσω τους γονείς μου, που κατα την διαρκεια των σπουδών μου βρίσκοντουσαν πάντα στο πλευρό μου, σε καλές και κακές στιγμές και πως αν δεν ήταν εκείνοι να με στηρίζουν όλα αυτά τα χρόνια δεν θα είχα καταφέρει τίποτα εως τώρα.

Ενα μεγάλο Ευχαριστώ

Contents

List of Figures

List of Tables

List of abbreviations

CRC	Combined Rogowski Coil
PRC	Planar Rogowski Coil
HF	High Frequency
WPT	Wireless Power Transfer
ADCs	Analog to Digital Converters
ENOB	Effective Number Of Bits
SINAD	Signal-to-Noise and Distortion Ratio
SAR	Successive Approximation Converter
CMR	Common-Mode Rejection
DNL	Differential Non-Linearity
LSB	Least Significant Bit
INL	Integral Non-Linearity

1. Introduction

1.1. Inductive charging

The wireless charging is based on the principle of electromagnetic induction, where conductive coils transfer power to each other wirelessly. It is a transmission form of energy by using electromagnetic oscillators [1].

For the operation of this system is necessary to have a transmitter and a receiver, whose basic function will be explained below. During the function, it does not need direct sight between transmitter and receiver. The Wireless energy transfer is a safe transmission method due to the short distance between of them.

Due to the fact that the wireless power transfer is based on electromagnetic fields, transmission of electricity and transmission of information can be achieved. Nowadays, the applications of wireless charging are at an advanced level.

1.2. History

However, the idea of wireless transfer energy is not new. Since 1890 Nikola Tesla had captured the imagination of the world with the invention of the Tesla coil, which could transmit wireless electricity. Thus, he constructed the famous tower of Wardenclyffe, 57 meters height, aimed at energy wireless connection between America and Europe. With this thinking, he gave a huge impetus to the development of wireless information transmission.

An overview of important milestones in efforts to transfer electric power wirelessly.

In 1821, it all started when the Danish physicist and chemist Hans Christian Ørsted discovered the phenomenon of electromagnetism.

In 1831, Michael Faraday discovered the principle of electromagnetic induction. This breakthrough came when he found that upon passing a current through a coil a momentary current was induced in another coil. This phenomenon is known as mutual induction.

In 1865, with the publication of the theory of the Electromagnetic field, James Clerk Maxwell suggested that electric and magnetic fields travel through space as waves moving at the speed of light. Maxwell proposed that light is an undulation in the same medium that is the cause of electric and magnetic phenomena.

Between 1886 and 1889, Heinrich Rudolf Hertz conducted a series of experiments that the same results as Maxwell theory about electromagnetic waves.

In 1888, Heinrich Herz bolstered the theory of Maxwell. Essentially this was the beginning of wireless power transmission.

In 1893, Nikola Tesla experimented with early X-ray technology, arc lamps and other new inventions. At the start of the 1900s, he built the famous Wardenclyffe Tower (1901–1917) which ended ingloriously because of insufficient funding [2].

1.3. Structure of wireless charging system

In Figure 1.1 the basic circuit operation of the wireless charging system which is intended for this work is presented. The system is divided into a primary coil which is fed by the distribution network and a secondary coil which is connected to the battery of the electric vehicle.

In the primary side, the power supplied from the distribution network and converted into a certain DC voltage through an inverter AC/DC. Then the DC/AC inverts the direct current to alternating current, which passes through the winding of the coil and generates a magnetic field connected to the secondary coil.

The secondary coil induces an alternative voltage, which will be reversed through the AC/DC converter to a direct current and will be corrected through the DC/DC converter to the desired supply voltage for charging the batteries.

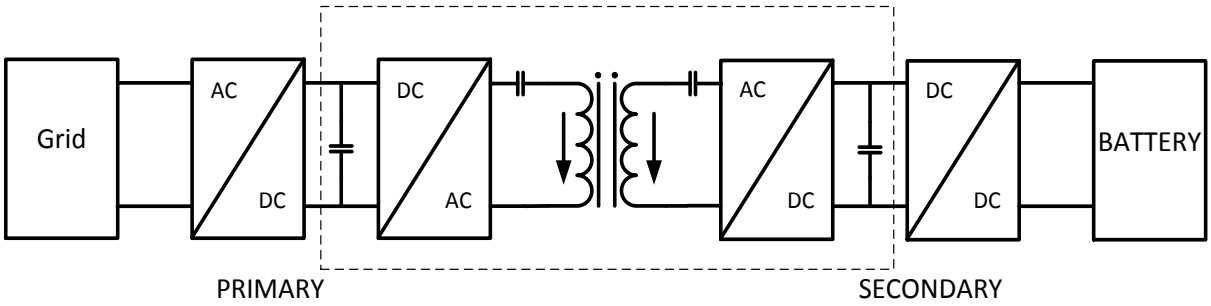

Figure 1.1 Structure of wireless power charging

The energy flows from a coil to another through the air gap in a distance that determined based standards. This function is based on the phenomenon of magnetic resonance, in which an object oscillates [1] when it receives energy of certain frequency. In this system, the coordination of electromagnetic radiation is exploited. Thus, there is a resonance system with highly efficient energy, which is achieved when the system operates. The transportable current produces magnetic and electric fields which extend up to a few meters around the device depending on the frequency. This magnetic field induces an electrical current in the induction system of each mobile device to the receiver coil with the same resonance frequency. Both circuits are coordinated together and then transfer the energy.

The system operation can be set in bidirectional power flow. When the energy flow is transferred from the primary to the secondary side, then the primary side operates as an inverter and the secondary side as a rectifier. In the opposite case, the flow of energy is transferred from secondary to the primary side, the secondary side operates as an inverter and the primary side as

a rectifier. With the ability of bidirectional power flow through the transformer, the leakage inductances store energy depending on the load requirement [3].

1.4. Description of the circuit being studied

In the present thesis, an effort is made for the measurement and the record of flow energy from one coil to another. For this reason, a sensor current in printed circuit board (PCB) has been designed and constructed., that will be placed in the DC/AC converter as shown in Figure 1.2, before the coils so that to recorded the alternating current.

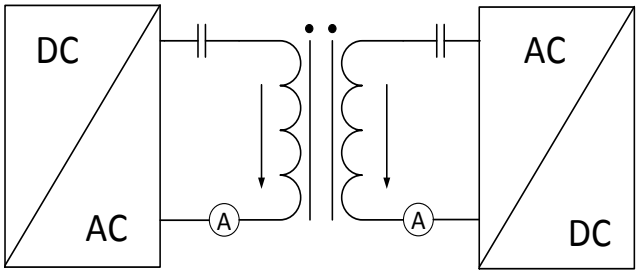

Figure 1.2 Inductive power transfer

It is perceived that, due to the oscillators of the system, the frequency of the alternating current will be high enough.

Due to this requirement and some further ones listed below, the study of all current sensor technologies takes place in order to find the most appropriate one so as to fit more in the particular application that will give the desired result.

The current sensor should provide good accuracy with low hysteresis, with fast responding to a high bandwidth and should have the high efficiency with the least possible losses. This combination is comprehensible that it cannot be provided equally well at all levels.

The intention in this work is to find a satisfactory and efficient combination of all these in a current sensor which will eventually be placed in the system. Moreover, all the elements that accompany a current sensor which is designed for a printed Circuit board (PCB) are studied, in order to be placed on one power converter.

1.5. Structure of the thesis

Based on the operation structure that was shown in Figure 1.3, the thesis is developed with a particular structure as shown below.

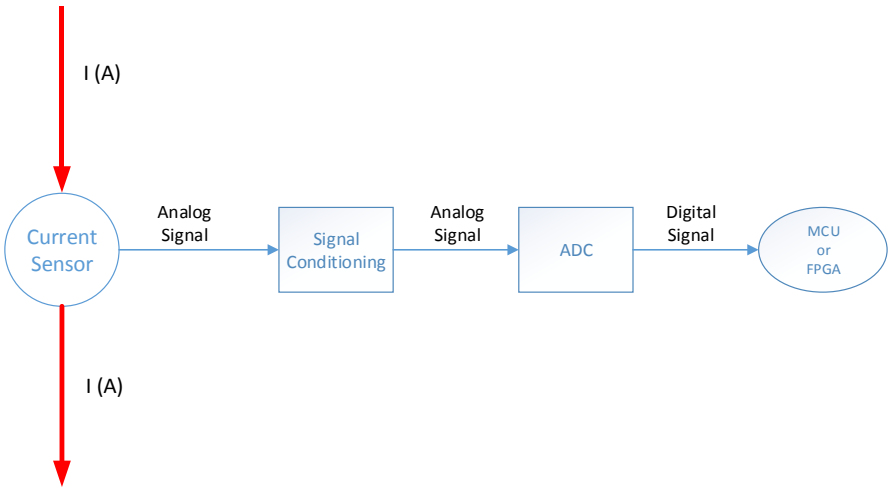

Figure 1.3 Structure of the system that is studied

In Chapter 2 the technologies of current sensors are examined. The features found on a data sheet are selected, as well as the way one can select each sensor based on the application. The operating principle of each technology is described and the advantages and disadvantages of the sensors are listed. Finally, a summary table with all the sensor technologies is presented.

In Chapter 3 examined the technologies of analog-digital converters (ADCs). Presented the features found on a data sheet and how can one select the each converter, based the application. Described the operating principle of each technology and referred the advantages and disadvantages of the ADCs. Finally, presented a summary table with all the ADCs technologies

Chapter 4 focused on the isolation of analog and digital measurements. A reference is made to the different isolation technologies and finally, a summary table with all the isolation technologies is made.

In Chapter 5 reference is made to the basic topologies of operational amplifiers. Analyzed these topologies and provided their equations.

In Chapter 6 summary of the technologies that were studied above was written and a rapprochement with their prevalent combinations of these topologies was attempted.

In Chapter 7, these applications have applied the results of experimental measurements of the circuit that designed and constructed in Altium design, whose construction is described in the Annex, are applied.

2. Technologies of Current Sensor

2.1. Introduction

The purpose of this section is to present the types of current sensors measurement technologies in a power electronic circuit with components that are commercially available.

A current sensor is a device that senses electric current (AC, DC) in a cable or a wire, and generates a signal. The produced signal could be an analog voltage or current or even digital output [4]. All the methods of measuring do not satisfy all the applications, for this reason, there are different sensor structures and methods to measure the current.

The input measurement current can be an alternating current or a direct current and the output signal can be an analog output, which duplicates the wave shape of the sensed current, bipolar output, which duplicates the wave shape of the sensed current, a unipolar output, which is proportional to the average or RMS value of the sensed current, unipolar, with a unipolar output, which duplicates the wave shape of the sensed current, digital output, which switches when the sensed current exceeds a certain threshold [4].

2.1.1. Main Industrial Technologies

Nowadays, over fifteen different types of designs and technologies are available and used for measuring electric current, depending on the application requirements, such as voltage and peak current, accuracy, bandwidth, cost, etc. These technologies are divided into six basic categories [5].

The main categories of current sensors are 1. Hall effect, 2. Current transformer, 3. Fluxgate sensor, 4. Rogowski Coil, 5. Shunt resistors, 6. Magnetoresistive sensors, which they will analyze in this chapter [6].

2.2. Main Parameters

These provisions which are described are the most widespread current sensors technologies. Depending on their operating mode, each sensor has its advantages and disadvantages compared to other technologies. For the selection of the appropriate instrument for a particular application, it is important to know the characteristics of the sensor about its performance and behavior during the measurement. The most important features listed below, are also those which determine the proper operation of sensors and this is mainly due to manufacturing reasons.

Compatibility in a sensor is the metric that describes whether the installation of the instrument will affect the values of the parameters to be measured. Ideal in terms of compatibility is considered an instrument that does not affect it at all.

The accuracy of a sensor is defined as the difference between the institution reading and the actual value of the measured magnitude. From the relation 2.1, we can calculate the maximum error contained in the indication, expressed as a percentage of the instrument indication. Practically all devices produce an error in their measurements and the challenge is for this error to be as small as possible. The accuracy depends on some factors such as hysteresis, the calibration, temperature etc.

$$\varepsilon_{\alpha}(\%)=\frac{(y_m-y_t)}{y_t}\ 100\% \qquad (2.1)$$

y_m: measured value

y_t: actual value

Calibration is defined as the process through which standard values input applied to a measuring system in order to the observation of the system output. Calibration essentially determines the range of the instrument.

The hysteresis is defined as the difference between the output of the sensor for a given input value x. This produces an error which affects the accuracy of the device (expressed in % of the output range). Also as hysteresis express the maximum input delay and the maximum output delay [7].

Saturation is the situation caused in a current sensor, when after a certain current input value exceeded the operating limits, then the sensor has an incorrect response, resulting in not show the correct value measurements.

The bandwidth of a sensor is defined by the maximum limits within which can be operated reliably. Usually, it is the range of frequencies as minimum and maximum value for which sinusoidal currents may be measured accurately 3dB of the specified sensitivity.

The sensitivity of a sensor is the minimum change in the input (x) of which is able to give a change in output. When the instrument has linear behavior then sensitivity is constant throughout the operating range.

Noise is caused during a measurement by external factors such as distance from a high frequency source voltage. The operating base of each sensor determines how affects the accuracy and granularity due to the noise.

Linearity is called the rate to which the graph of the output relative to the sensor input approximates a straight line. A sensor can be linear for the range of value.

The resolution is defined as the minimum amount of change of the measured size of the sensor which leads to a distinct change in output, expressed as a percentage of the range of the measured size.

$$resolution\ (\%) = \frac{\Delta x}{r_i}\ 100\% \qquad (2.2)$$

If the input is increased from zero, there will be some minimal smallest value of which there will be no distinct change in output. This minimum value determines the threshold of the instrument.

2.1. Hall-Effect

The Hall Effect current sensor based on the phenomenon of Hall which is caused by the Lorentz forces. A thin semiconductor material plate leaking from the current *I* (Figure 2.1). The moving electric loads of current, affected by an external magnetic flux *B* that generates a Lorentz force perpendicular to the current direction. This results in the diversion of the current and the generation of electrical loads at the ends of the plate, creating there a potential difference, which is called voltage Hall V_h [8]. As long as no applied magnetic field in the semiconductor material, the voltage across the element will be zero [9][10].

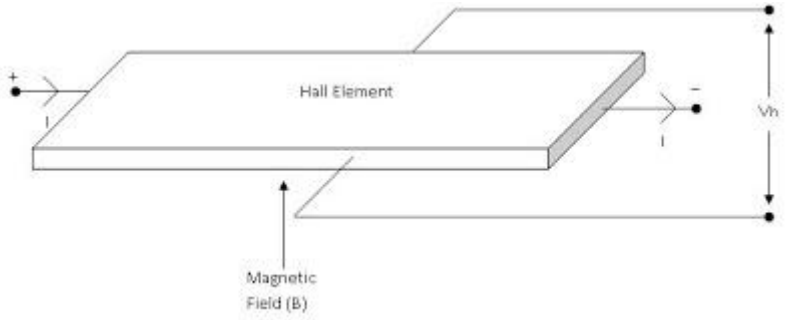

Figure 2.1 Hall Effect [9]

The Hall voltage is defined by the following relationship.

$$V_h = \frac{I\ B\ d}{n\ q\ A} \qquad (2.3)$$

I: The current that passes through the plate

B: The intensity of the magnetic field- the width of the conductor

$1/n\ q$: Firmly Hall of conductive plate

$A = t\ d$: Where t is the thickness and d is the width. Rewrite the equation:

$$V_h = \frac{I\ B}{n\ q\ t} \tag{2.4}$$

With sensors which make use of this phenomenon, it is possible to measure the current AC, DC and induction [10] The two most commonly types of Hall transducer are the open loop and the closed loop.

2.1.1. Open Loop

The open-loop sensor is the simplest application of the Hall Effect. The structure of the sensor shown in Figure 2.2. A conductor which is flowing from current produces a magnetic field that is concentrated in a magnetic core. In the magnetic core, there is a gap in which is placed the Hall plate, in order to measure the density of magnetic flux created in the gap. The Hall plate is powered by direct current I_c from the electronically integrated circuit in the sensor. In the linear area function of material, the magnetic flux density, *B*, is proportional to the primary current I_f and the Hall voltage, V_h is proportional to the flux density [10].

The primary current is measured without electrical contact with the circuit providing galvanic isolation. The Hall voltage is given by the equation 2.5 [8].

$$V_h = k\ I_c\ B \tag{2.5}$$

In the linear area function of material, the magnetic flux density, *B*, is proportional to the primary current I_f and the Hall voltage, V_h, is proportional to the magnetic flux density *B*. This voltage is the electrical signal output of the sensor [10].

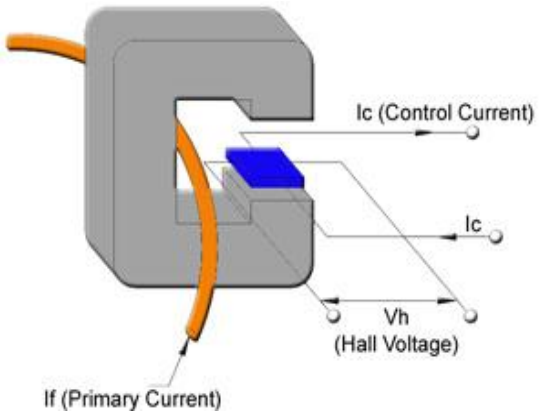

Figure 2.2 Open Loop Hall Effect [8]

The output signal of the Hall device, V_h is then further amplified by additional internal signal conditioning circuitry to provide an instantaneous output voltage proportional to the primary

current [8]. The output signal is compensated to removed the offset and the effects of temperature and enhanced if it is less than desirable. The output of a open loop sensor is proportional to the measured current.

The open loop current sensors are suitable for measurements of AC and DC currents. These sensors are used in applications which don't require high accuracy level. Over of the 100 kHz, the inductive or capacitive sensor output begins to distort. Due to the fact that the open loop can be interjected by an external magnetic field. It offers galvanic isolation and due of their simple construction are small, lightweight and low cost. Also, it has low power consumption.

2.1.2. Closed Loop

The closed-loop sensors have a similar circuit with the open loop, the difference being that there is an addition compensation circuitry winding on the magnetic core which increases the performance of the operation. The field in which the plate is positioned in this provision. It comprises two separate fields. A field created by the current measure as in open loop configuration and an even field from the secondary winding core. The value of the Hall voltage appearing at the sensor, processed by a controller which in turn produces a voltage at the secondary winding. The voltage produced by the secondary winding to create a field equal and opposite to that which existed [10]. The end result is a magnetic flux in the sensor core is constantly controlled at zero [11]. In this way, the secondary current I_s is identical to the current I_0 measured and normalized by the ratio of turns of the two windings. In sum, the secondary current, Io, creates flow equal measure but opposite direction from the flux created by the primary I_f.

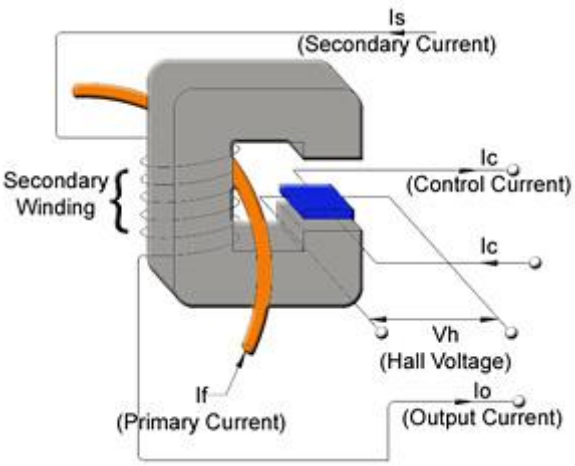

Figure 2.3 Close Loop Hall Effect [8]

The amount of current required to balance zero flux is the measure of the primary current flowing through the conductor in time, multiplied by the ratio of the primary conductor to secondary windings.

$$I_0 = I_f \, dt * \frac{1}{N_s} \tag{2.6}$$

Placing a resistor measuring R_m in series with the secondary winding, created an output voltage proportional to the measured current.

$$V_{out} = R_m \, I_0 \tag{2.7}$$

The closed loop sensors are suitable for AC and DC current measurements and offer galvanic isolation. Their design provides a good accuracy and linearity due to the winding compensation. Furthermore, the secondary winding will act as a current transformer at higher frequencies, which significantly increases the bandwidth and reduce the response. Another advantage you have is that it is suitable for noisy environments.

The main disadvantage of these sensors is the power consumption due to the resistor from the power supply side of the secondary. They have a larger size than the open loop and are more expensive to manufacture.

2.2. Fluxgate Sensor

The Fluxgate current sensor design is described as a structure similar to the closed loop Hall Effect, using the same magnetic circuit with the difference in construction that replaces the Hall plate with a Probe coil (saturable inductor) comprising the secondary winding, as shown in Figure 2.4 [8]. The detector is made of separate pieces of high saturated material.

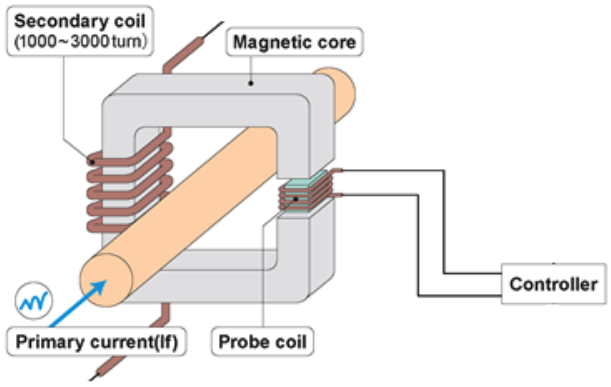

Figure 2.4 Fluxgate Current Sensor [8]

As in operation of Hall Effect closed loop, so here the flow of the magnetic field in the gap should be zero. Now, this work undertakes by the secondary winding located on Probe coil [12].

The current I_f of the primary conductor generates a magnetic field in the vacuum of magnetic core, which is also detected by Probe coil. However, the Probe coil generates in the core of a second magnetic flux too. The sum of these two magnetic flow produces an over-saturation of the saturable inductor's core and its inductance drops. The design of saturated Probe coil provides high saturation induction, the total flux close to zero and a low inductance below saturation. Then we apply the function of closed loop where changes in the induction created by the primary current are detected and compensated [12].

This sensor is suitable for measurements of AC and DC currents. It offers galvanic isolation, high accuracy, linearity and sensitivity, wide range and fast response. Also, the operation of it is not affected by external noises.

Sensors of this type are very expensive. They have great power consumption and the design is complicated.

2.3. Current Transformer

The principal of the operation of a current transformer is no different from that of an ordinary transformer, except that the magnetic flux created by the current in a primary input [13]. A current transformer (CTs) consists of a magnetic core and two inductive coils which are magnetically linked. The first coil is called primary and second is called secondary. The two inductive coils are galvanic isolated. When in a primary input connected an AC source then an alternating flux created in the core. This magnetic field induces a proportional current in the secondary winding [6]. Thus, according to a Faraday law of electromagnetic induction, a mutually induced (M) electromotive forces (EMF) had produces between coils [14].

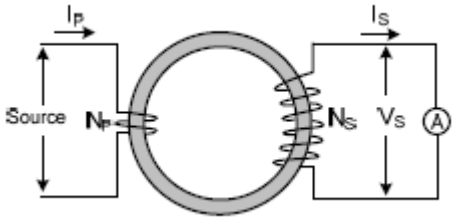

Figure 2.5 Current Transformer [14]

The magnetic field induces a proportional current in the secondary winding. A burden resistor required to convert the current to a voltage signal for further processing in an ADC [6]. This is not affected the function in low current applications but is often impractical for high current applications. The resistor in the electronic circuit consumes a lot of power, unless the resistor is very low in value, in which case there may be very little voltage to measure. The resistor could be excessively large. The resistor's heat may affect the resistor value, thereby reducing the accuracy of the measurement [8].

In an ideal transformer, the induced secondary electromotive forces (EMF) is same as the secondary voltage V_s. The equation between the primary and secondary side, given by:

$$\frac{V_p}{V_s} = \frac{I_s}{I_p} = \frac{N_p}{N_s} \tag{2.8}$$

V_p: Primary Voltages

V_s: Secondary Voltages

I_p: Pripary Currents

I_s: Secondary Currents

N_p: Number of Primary Turns

N_s: Number of Secondary Turns

With their function as CTs reduce high currents to a much lower value and provide a convenient way of monitoring the actual electrical current flowing in an AC line [13]. The accuracy of CTs depends on the mechanical tolerances of the setup, burden accuracy and temperature drift of the magnetic core. The saturation level of the magnetic core limits the dynamic range of a CTs [6].

A current transformer measures AC currents. It features galvanically isolate and provide a satisfying bandwidth. Due to the magnetic core, the sensors of this type is quite bulky in size. They have core losses and resistance losses in the secondary circuit. In large currents observed thermal drift.

2.4. Rogowski Coil sensor

The Rogowski Coil is an electrical device used for measuring alternating current. The operation of the Rogowski coil is based on Faraday law. The total electromotive force induced in a closed circuit is proportional to the change of magnetic flux in time [15].

The structure of the Rogowski coil is similar with this of a CTs, with the difference that is missing a magnetic core and the work becomes from the helical winding coil of N turns, on a non-magnetic air core of constant cross-sectional area, as shown as in Figure 2.6 [16].

The uniformly wound coil on a nonmagnetic material of constant cross-sectional area is formed into a closed loop. The winding wire is returned to the starting point along the central axis of the former. The free end of the coil is normally inserted into a socket adjacent to the cable connection in a way that allows it to be unplugged thus enabling the coil to be looped around the conductor carrying the current to be measured [17].

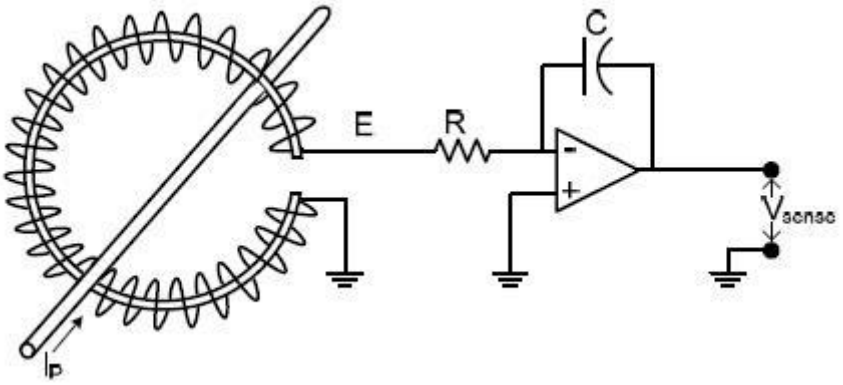

Figure 2.6 Rogowski Coil current sensor [14]

An AC current I_p flow in a conductor which passes within the Rogowski coil, develops a magnetic field and the interaction of this magnetic field and the Rogowski coil local to the field gives rise to an induced voltage within the coil which is proportional to the rate of change of the current being measured. Provided that the coil constitutes a closed loop, the voltage induced in the coil is proportional to the rate of change of current. It may be shown that the voltage *E* induced in the coil is proportional to the rate of change of the encircled current *I* according to the equation 2.9. Where *M*, the mutual inductance of the circuit and *di/dt* is proportional to the time derivative of current flowing the conductor [18][19][20].

$$E = -M\frac{d_i}{d_t} \tag{2.9}$$

The mutual inductance *M* depends on the geometric parameters of the Rogowski coil.

$$M = \frac{\mu_0 A N}{l} ln\left(\frac{b}{a}\right) \quad (2.10)$$

μ_0: is the permeability of air

N: is the numberof turns of coils

l: is the width of the toroid in meters

a, b: is the inside and the outside diameter in meters respectively.

The Rogowski coils measure AC current. Due to the absence of a magnetic core, it offers galvanic isolation. Large currents can be measured without saturation and remain in the linear area of measurement. They present a wide range of power measurement and frequency. The Rogowski coils have low manufacturing cost.

A disadvantage is the fact that the output signal has to pass through an integrated circuit to increase the output signal, in order to observe the waveform of the current.

2.5. Shunt Resistors

Another method is known as the shunt resistor. This technique is simple in operation, with the current flows through a high precision resistor with a low resistance value [21]. The resistance value depends solely on the magnitude of the current to be measured [22].

A shunt resistor can be designed into many ways. The basics operation is this which showing in Figure 2.7. The two edges of the resistance are connected with a difference amplifier the which will convert the signal to desired levels in order to be connected to the ADC specifying a shunt resistor [21].

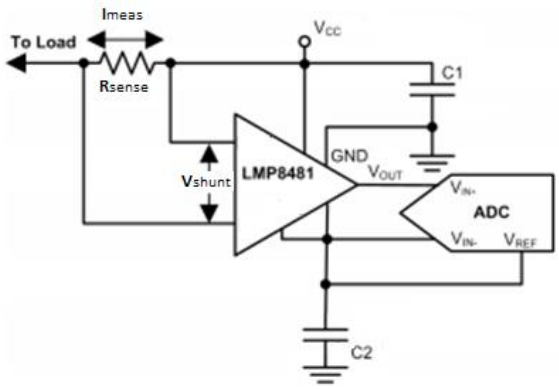

Figure 2.7 Circuit of shunt resistor[3]

A current *I* flows through the shunt resistor which causes a voltage drop at the ends of shunt resistor. Knowing the value of *R* shunt and measuring the voltage drop *V* shunt in *R* shunt with a parallel electronic circuit, by the Law of Ohm's is now calculated the value of the current. The bellowing equation applies to the measurement of voltage in the *R* shunt [23].

$$Imeas = \frac{Vshunt}{Rsense} \tag{2.11}$$

The voltage drop in low-ohmic resistors is respectively small. For this reason, externals signals can create error voltages and change the measured result. For this reason, it needs careful layout design [24].

The shunt resistor current sensor can measure AC and DC current. The measurement range is not for very high currents. Offers high measurement accuracy and a very good bandwidth. It has a low manufacturing cost.

The main disadvantage of this topology is the design complexity. Due to the voltage drop in the ends of the shunt resistor needs a circuit by amplification, which limits the accuracy and changes the bandwidth [25].

An added disadvantage is that it does not provide galvanic isolation. This problem can be solved either by designing a galvanic isolation after an ADC [26], that offers inside galvanic isolation and seems an ideal solution for the specific application.

High temperatures negatively influence the accuracy of the shunt resistor. The high temperatures negatively influence the accuracy of the shunt and observed thermal drift [21]. Also is a noisy topology which affected by external noises.

2.6. Magnetoresistive Sensor

Magnetoresistance (MR) is the property of a conducting material to change the value of its electrical resistance when an external magnetic field is applied to it [4]. This effect occurs in ferromagnetic materials (nickel-iron), whose specific impedance changes similarly with the direction of a magnetic field which applied on it [27].

Due to the high sensitivity and high accuracy that this sensor has, the MR sensor does not require the use of an iron core for produce a magnetic field to the circuit but generated by the conductor which flowing the current. The MR sensors don't suffer from hysteresis and have a high bandwidth [27].

Depending on the material used, there are two types of magnetoresistive sensors:

Anisotropic magnetoresistance (AMR) sensors use ferromagnetic materials in which a magnetic field influences the electrical resistance. The resistance variation is very small therefore, Wheatstone bridges are often used to sense it [6].

Giant magnetoresistance (GMR) sensors rely on a significantly higher impact of the magnetic field on the resistance of a structure built of alternating ferromagnetic and nonmagnetic layers. The GMR sensors have more sensitivity than AMR, the production process is more complex and expensive [6].

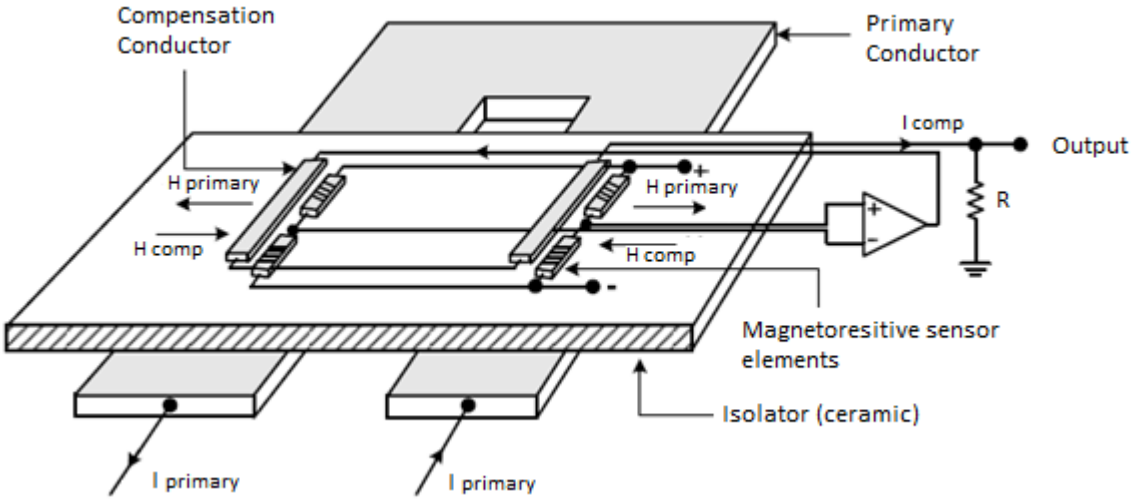

Figure 2.8 Magnetoresistance [28]

This effect, found in ferromagnets, depends on the orientation of the magnetization with respect to the electric current direction in the material [29].

A differential magnetic field must be measured, which is the field gradient created by two currents with opposed flow directions. Four MR resistors are connected in a Wheatstone Bridge to form a complete AMR sensor. The resistors are placed so that they represent a differential field sensor. With this way decreases a temperature drift, the interference fields eliminated and doubles the signal output. Applying an input signal, a magnetic field occurs which change the

values of the resistors, generating an output signal proportional to the magnetic field strength. The chip takes place on a ceramic substrate, combined with a processing circuit and a signal conditioning [13][27].

The magnetoresistance sensors measure AC and DC currents. Feature inherently low hysteresis and high linearity in the measurement accuracy. They have the extremely high bandwidth and can to detect magnetic fields with frequencies in the MHz region. They have high sensitivity. It provides galvanic isolation [30]. They are small in size and easy to design application. The cost of it is satisfactory.

Their disadvantages are that they are sensitive to external noises. Also, a very strong magnetic field may damage the sensor. The exhibit thermal drift and they have limited linear range [9].

2.7. Comparison of Current Sensors

The sensors that are used usually not combine all the features at a satisfactory level. For example, a sensor can offer high precision and sensitivity but it can be expensive. Table 1 shows the comparison of these sensors on the main levels.

Details/Sensors	HALL EFFECT		FLUXGATE SENSOR	SHUNT RESISTORS	MAGNETORESITIVE SENSOR		ROGOWSKI COIL	CURRENT TRANSFORMER
Measurement Current	AC/DC		AC/DC	AC/DC	AC/DC		AC	AC
Core	Yes/No		Yes	No	No		No	Yes
Current Sensor Type	Open Loop	Close Loop	Close loop	-	AMR	GMR	Close Loop	-
Accurasy	Low	Medium	High	High	Medium	High	Medium	Low
Bandwith	20kHz - 800kHz		<1 MHz	<1 MHz	>2MHz		>1MHz	<1MHz
Saturation and Hysteresis problem	Yes		Yes	No	No		No	Yes
Linearity	Low		Medium	High	Medium		High	Low
Isolation	Galvanic		Galvanic	-	Galvanic		Galvanic	Galvanic
Current Range	Medium		Medium	Low	Medium/High		High	Medium
Thermal Drift	Yes		Yes	Yes	Yes		No	Yes
Loss	Medium		Medium	High	Medium		Low	High
Size	Small		Small	Small	Small		Normal	Big
Cost	Cheap	Normal	Expensive	Cheap	Normal		Cheap	Normal

Table 1 Comparison of Current Sensors

Most sensors have the ability to measure AC and DC currents. Unlike the Rogowski Coil sensors and Current transformer which due to their particularity, they measure only AC.

The sensors are separated in sensors with magnetic core and sensors without a core.

The sensors with the core as shown in Table 1, to the continuous high current operation, the core begins to saturation and hysteresis resulting in deviations from the actual measured value.

Even at high current flow, the magnetic core begins to heat with a resulting thermal drift leading to large losses in the core. Even at high current flow, the magnetic core begins to heat with a resulting thermal drift which leading to large losses in the core. The sensors without magnetic cores do not present the disadvantages of sensors with core except in some cases where there is thermal drift, which has to do with the sensor material.

Another separation of the sensors has to do with whether they are an open or closed loop. Generally, the closed loop sensors have better accuracy due to the compensation winding which does not allow the circuit is affected by external factors such noise and unwanted signals, resulting in better precision in measurement. In contrast to the other sensors that some of them are open loop, can interfere with external magnetic fields and distort the measured current flow, resulting error in a measurement.

In all sensors except the Shunt resistor, the measurement of currents is done by the method of induction currents so offers galvanic isolation.

In the most sensors, the bandwidth is limited up 1 MHZ, which price is satisfactory for measurement of currents. The magnetoresistive sensors appear bigger bandwidth from the manufacture them than the rest except the Rogowski coil which can be designed in a high bandwidth, depending on requirements.

The size of the sensors depends mostly on the material being manufactured. For this reason, the Shunt resistor has a smaller size compared with the others. The sensor with the largest bulk is the current transformer. In most sensors as a Rogowski coil, Fluxgate sensor and Hall effect, the size of the sensor is independent of the current to be measured, because the modification has to do with the electronic circuit that accompanying it and not on the size of the sensor. In the case of the Rogowski Coil, currents from a few mA up to currents of kA can be measured equally well with the same circuit with minimum heat loss.

The cost of the sensors depends on the application intended. But in general terms, the Fluxgate is the most expensive by far than the others and this is reasonable considering the circuit which it offers.

3. Sampled Data Systems

In a data collection system, a signal input from a source is needed and the convert of it into a digital signal so that signal can be processed. Usually, the analog signals as we saw in the previous chapter are derived from sensors that perceive the real sizes and convert them into electrical signals. With the help of a converter, the signals are digitized [31].

The steps followed for an analog signal to digital conversion system are as follows:

• Analog Multiplexer and Signal Conditioning

• Sample/Hold Amplifier

• Analog-to-Digital Converter

• Timing or Sequence Logic

3.1. Analog to Digital Converters

The Analog to Digital Converter (ADCs) is a system that converts an analog voltage or current to digital output signal binary numbers form of n-bits, does the conversion periodically, sampling the input for the further signal processing [32].This number is a binary fraction which represents the ratio between the unknown input voltage and full-scale converter $V_{FS} = k\, V_{REF}$, where V_{REF} is the reference voltage with which the ADCs operates and the k determines the gain voltage of the converter and is usually equal to the unit. The equation governing the input voltage with the output binary code given [33] by:

$$V_{REF}(b_1 2^{-1} + b_2 2^{-2} + \cdots + b_N 2^{-N}) = V_{in} \pm V_x \tag{3.1}$$

Where

$$-\frac{1}{2}V_{LSB} \leq V_x \leq \frac{1}{2}V_{LSB} \tag{3.2}$$

As VLSB defined the difference in voltage when the binary code change by one LSB (Least Significant Bit) or else less significant digit:

$$V_{LSB} = \frac{V_{REF}}{2^N} \tag{3.3}$$

From the above equation, we conclude that a variety of input values produce the same digital output word. This is the representation of the analog value by a finite number of bits and it is called a quantization error [33].

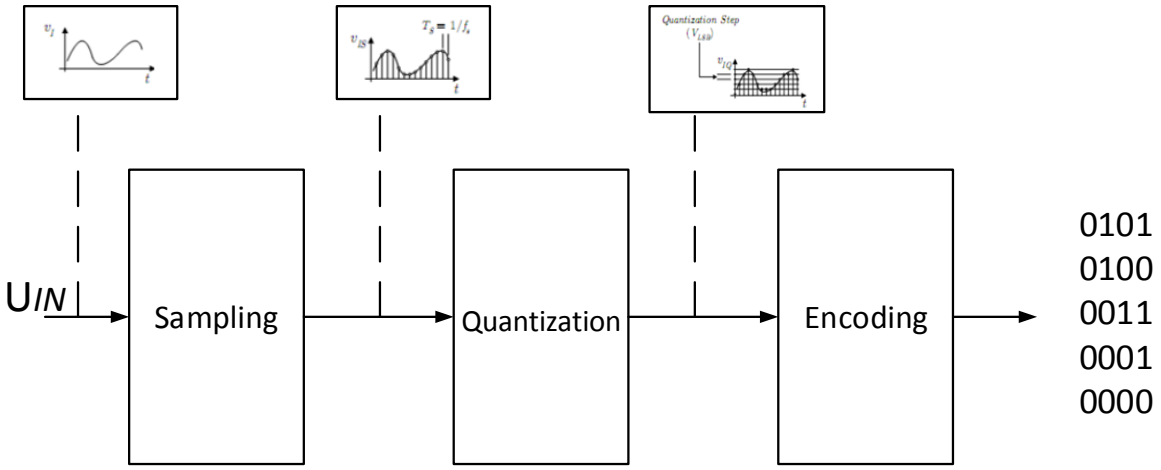

Figure 3.1 Basic operation of an ADCs

A complete analog-to-digital conversion system includes three main stages as shown in Figure 3.1. First, the analog signal must be discrete in time, this process is called sampling and is controlled by the clock signal [34]. Then becomes the quantization where the analog signal quantized in the final stage of the conversion is the encoding of the signal at the output of the ADCs converter which gives a binary coded representation of the quantized signal

3.2. Sampling Rate System

To produce a digital signal from an analog input signal, should the analog signal to be processed. The first step of the signal processing is the sampling, as shown in figure 3.1. The analog signal is converted into a plurality of discrete values, between the given limits of the total change. The process of a real-time sampling system is shown in Figure 3.2. This signal takes a sampled at time T, which called the sampling period and the each value, represented by black dots in figure 3.2. In all architectures, high-speed converters, in the input is sampled once per clock period. In this way, the clock frequency corresponding to the sampling frequency [34].

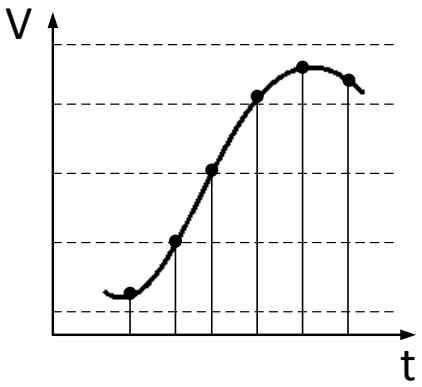

Figure 3.2 Sampling and quantization levels of digital signal

This process causes changes in the spectrum of the original signal and is called sampling. To allow retrieval of the original signal from its samples, according to the Nyquist sampling theorem, the sampling frequency must be at least twice the maximum frequency of the signal. To be the precise conversion of the analog signal should not change the duration of the measurement. However, most natural signals varied in time with a rhythm. The percentage change is likely to cause the wrong measurement, for this reason, must bear one sampling step and retention (Hold), thus its output gives the instantaneous value of the analog output [35].

3.3. Quantization

The most important component in an ADC converter is that their input is analog and the signal output is in digital form, therefore the signal outputted from the converter quantized. Quantization is the process of approximation of an analog sample with a finite number of bits. With the quantization limited the range to a set of a finite number of M values. The clarity of the signal depends on the number 2^N where n number of bits [33]. A digital N bit size may have only 2^N possible states. As a result, an N-bit converter can only have 2^N possible digital outputs. This fact of the restriction of values which can be produced by an ADCs converter called resolution. The resolution of ADCs converters can be expressed as the Least Significant Bit - LSB, in parts per million Full-Scale - ppm FS and in millivolt (mV). Figure 3.3 shows an example of quantization with ideal transfer characteristics in a monopolar converter size 3 bit. Therefore, the transfer characteristic comprises from 2^3= 8 horizontal steps. When considering the displacement of the gain and the linearity of the [36].

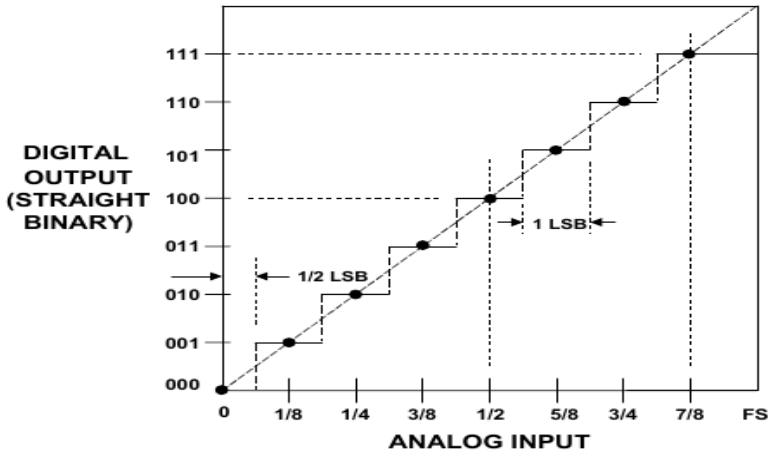

Figure 3.3 Quantization an analog signal [36]

Figure 3.3 shows the quantization process, wherein the quantization step (q) converts the amplitude of the input signal to a binary number. Thus the signal divided into intervals which called steps width LSB, which is the numeral bits corresponding to a quantization level, between two reference voltages. The accuracy of conversion depends on the number of quantization levels. This number determines the number of output bits. The output voltage of the circuit approaches the nearest quantization level as shown in Figure 3.3. Therefore, the quantized signal

is an approximation of the original signal [34]. The quality of the approximation can be improved by reducing the size of the steps, and thus increasing the number of fixed stations. The difference shows the output of the quantizer from the original signal can be considered noise in the quantization process is called quantization noise [37].

And the RMS value of this error is given by the equation:

$$V_{qRMS} = \sqrt{\frac{1}{T}\int_{-\frac{T}{2}}^{\frac{T}{2}} V_q dt} = \sqrt{\frac{1}{T}\int_{-\frac{T}{2}}^{\frac{T}{2}} V_{LSB}^2 \left(\frac{t}{T}\right)^2 dt} = \frac{V_{LSB}}{\sqrt{12}} \quad (3.4)$$

Where from the equation 3.4, shows the dependence of the number of bits of the converter. Also, we observe that the noise power is reduced by 6 db for each additional bit in the ADC [33]. The signal to noise ratio (SNR), which measures the noise level, can be calculated from the follow equation, where n is the number of bits used on the ADC:

The noise level can be calculated from the ratio of signal to noise, from the following equation. Where n is the number of bits.

$$SNR = 6{,}02n + 1{,}76dB \quad (3.5)$$

The higher the SNR, the better. For example, an 8-bit ADCs provides a SNR of 49.9 dB, while a 16-bit SNR provides a SNR of 98 dB [38].

3.4. Encoding

In the final stage of the conversion is the encoding of the signal, which follows the quantization of analog signal, on the output of the ADCs. The encoding gives a binary representation of the quantized signal. So with sample width of 8 digits, the signal may have 256 different levels.

3.5. Main parameters of ADCs

This section lists the most important parameters that determine the proper operation of an ADCs and are mainly due to manufacturing reasons.

Resolution: Defined as the number of discrete analog voltage levels corresponding to different digital words. Consequently, a converter with N-bit resolution can recognize 2^N different analog levels. The analysis should not be confused with the precision of the converter. It refers only to the number of bits which has available [32]. To have more accuracy in the analog signal, the resolution must be an increase. An ADC with higher resolution reduces the quantization error [39].

Offset error (E_{off}) is the error due to the superposition of a DC voltage in the input voltage of the ADC.

$$E_{off} = \frac{V_{0\ldots01}}{V_{LSB}} - \frac{1}{2}\ \text{LSB} \tag{3.6}$$

Full-Scale Error: In an ADC it is observed that it reaches gets the maximum digital value although the analog input has not got the maximum value. This error is called Full-Scale Error is expressed in LSB.

Gain error (E_{gain}) is the deviation of the slope of the transfer function from that of the corresponding ideal ADC.

$$E_{gain} = \left(\frac{V_{1\ldots1}}{V_{LSB}} - \frac{V_{0\ldots01}}{V_{LSB}}\right) - (2^N - 2) \tag{3.7}$$

Integral non-linearity (INL): Defined as the maximum conversion error, after deduction of the Gain and Offset Error. In ADC represents the deviation of the transition points of the code from their ideal positions.

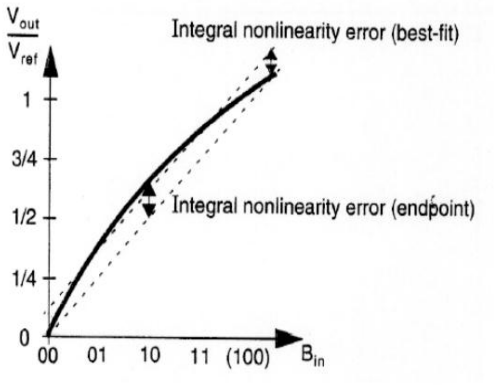

Figure 3.4 Integral non-linearity error [40]

Differential non-linearity (DNL): When the binary input is altered 1 bit, then the output voltage will be changed by 1 LSB. The DNL is the maximum difference between of any step of the inverter output and the ideal step size of 1 LSB. For the ADCs is the maximum fault that can be observed from level to level [40].

The sample rate is determined in samples per second (sps). Sample rate is the rate at which an ADC gets samples from the analog input. For few ADCs that achieve one sample per conversion, the sampling rate is stated to as the throughput rate [39].

The Dynamic Range is defined as the ratio of the RMS value of a sine to the RMS value of quantization noise plus distortion. Usually expressed in dB [39]. For the ideal converter dynamic range [33] is:

$$\frac{V_{in(RMS)}}{V_{q(RMS)}} = 20\log\left(\frac{V_{REF}/\left(2\sqrt{2}\right)}{V_{REF}/\sqrt{12}}\right)0 = 6.02\text{bits} + 1{,}76\text{db} \tag{3.8}$$

Effective Number of Bits (ENOB) identifies the dynamic performance of an ADC at a particular input frequency and sampling rate. An ideal ADCs error consists exclusively of quantization noise. For a full-scale sinusoidal input, waveform is calculated from the following [39] equation:

$$\text{ENOB} = \frac{\text{SINAD} - 1{,}76}{6{,}02} \tag{3.9}$$

Accuracy or else maximum integral nonlinearity error, usually expressed as a percentage error of the full scale, as the number of active bits (ENOB) or as a fraction of an LSB. Divided into absolute and relative. As absolute accuracy is defined, the difference between the ideal and the actual response. Includes offset, gain and linearity errors. As relative accuracy defined the accuracy, which having removed the offset and gain errors. Accuracy greater than the Resolution, it shows that the characteristic of the inverter is very accurate [32].

Signal to Noise And Distortion (SINAD) is the ratio of the RMS value of the sinewave in the input, to the RMS value of the converter noise plus distortion (without the sinewave). RMS noise plus distortion includes all spectral components up to the Nyquist frequency, excluding the fundamental and the DC offset. SINAD is typically expressed in dB [39].

3.6. Architectures of Converters

In this section, a description of the operation of the most popular topologies of ADC is attempted.

3.6.1. Flash ADC

The Flash ADC or Parallel ADC is the simplest circuit to understand the operation of an ADC. This ADC consists of a series of high-speed comparators, each one comparing the analog input signal to a reference voltage. For an N-bit ADC converter, the circuit uses 2^N-1 comparators. The reference voltage (Vref) is a constant voltage provided by a voltage regulator. The reference voltage provided to comparators from a divisor with 2^N resistors. When the analog input exceeds the reference voltage of each one comparator, then the comparators output produces 1, in the otherwise, the comparator output will be 0. The following figure shows a Flash ADC circuit [41] [42].

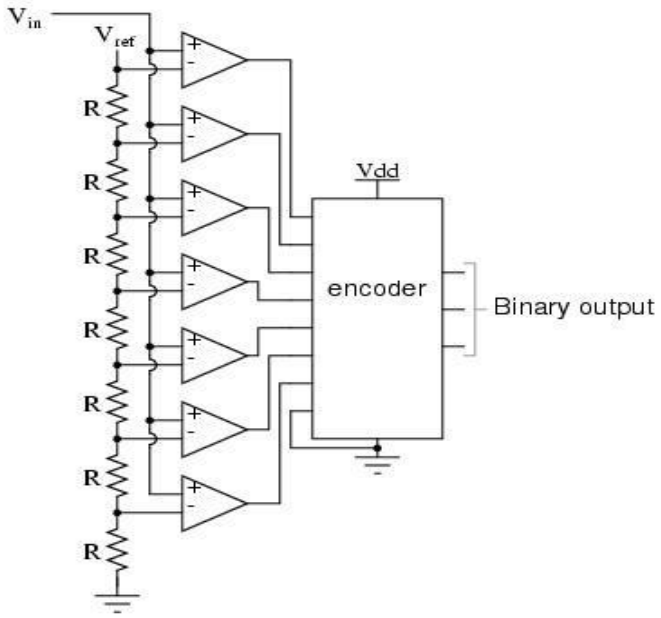

Figure 3.5 Flash ADCs [41]

The encoder circuit connects to the comparator outputs, which produces a binary output.

The Flash converter, apart from the simple construction and the effectiveness with regards to speed, also has a major disadvantage, which is the restriction to the comparator and the gate delay. For example, a four-bit version would require $2^4 - 1 = 15$ comparators. With each additional output bit, the number of required comparators doubles. Taking mind that 8 bits are considered the minimum for each ADC (255 comparators) [41]. Due to this disadvantage, the inverter has developed into Flash converter two steps, which reduces the number of comparisons

with quantization of an input in two stages. The activated reduction factor in the number of comparisons in compared to the Flash ADC is exponentially proportional to the resolution of the converter. This shows, as much as higher is the resolution so the more area efficient it becomes to use this topology [43].

The advantage of this converter is that it is the fastest ADCs to convert the signal for high bandwidth applications. The main disadvantage of their converter is that it needs many parts (255 comparators for 8-bit ADCs) resulting in consuming a lot of power, it has a relatively low resolution and can be quite expensive.

3.6.2. Pipeline ADC

The basic function of Pipeline ADC is similar to the Two-Step Flash. Each stage of quantization Nj -bits, j = 1, 2, ..., K (NJ <N), generate an amplified residue for further quantization which performed by subsequent stages. This converter has the advantage that during the quantization of the first stage does not need to come to an end so that it can be quantized next stage, this applies to all other stages except the first stage. This means that when the ADC starts its operation then all stages are processing data. In this way, the performance of Pipeline ADC is close to Flash ADC [43].

The pipeline ADC can be designed in many different ways, it depends on the number of bits per stage, the number of stages, number of correction bits and the timing. In Figure 3.4 we see one of the most popular designs, a track-hold (T/H) circuit, an n-bits ADC and a digital to analog converter (DAC) n-bits, which do the reverse process of the ADC.

Initially, the input signal quantized is n-bit ADC the result of which is converted to analog by the N-DAC bit and is subtracted from the original input voltage. The result of the subtraction moves to the next stage where the same procedure [44].

The track-and-hold which is shown in figure 3.4, plays the role of an analog delay line, which is configured to enter hold mode when the conversion of the first stage is complete [45].

The pipeline ADCs is fast and satisfying applications requiring high bandwidth. Disadvantages of this converter are the low resolution, the Larger cycle latency [44], and several high energy consumptions.

3.6.3. Delta-Sigma ADC

Another technology in the field of ADC is the delta sigma. The delta sigma operates as a converter voltage-frequency, by performing quantization of the analog input signal. The delta sigma provides at its output a pulse train of 1 and 0 with a period $t = 1/f_q$, where f_q is the oversampling frequency [46].

The input of ADC is fed from an analog voltage, which is linked to an integrator, so bring the signal into the desired form. this voltage is compared with the ground potential (0 Volt) with help of a comparator. The comparator is essentially an ADC 1-bit producing 1 bit to output (0 or 1), depending on whether the output of the integrator is negative or positive. The output comparator Q of a flip-flop is clocked at high frequency and returns back to the integrator to drive the integrator towards zero volt output. The circuit as shown as in the figure below [47].

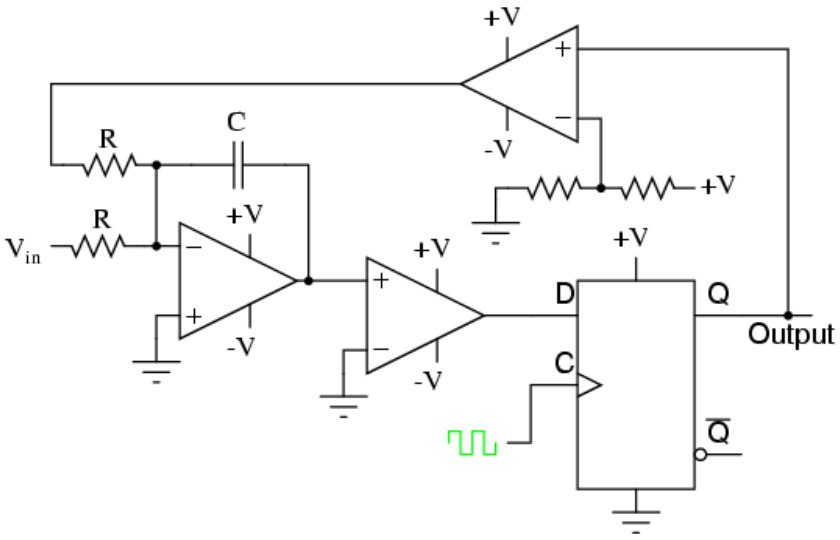

Figure 3.6 Basic circuit of Delta Sigma ADC [47]

As shown in Figure 6, the input voltage *Vin* is connected to an op-amp which is the integrator circuit, wherein the output signal feeds comparator. The output signal of the comparator (1-bit) is driving to the input D of the flip-flop, which latched in each pulses clock C, sending either 0 or 1 signal to comparator who is located after the Q output of Flip Flop. This comparison is necessary to convert the unipolar output voltage 0V / 5V to a voltage signal + V / -V to return to the integrator. In summary, the first comparator detects a difference between the integrator output and zero voltage. The integrator sums the comparator's output with the analog input signal [47].

This converter is mainly used in applications that do not need high speed but required high accuracy and resolution. Due to the oversampling, this converter is one of the slower converters and has high latency. It has low power consumption and is a good solution for low-cost applications.

3.6.4. Dual Slope (Integrating) ADC

An integrating ADC for converting the input voltage to digital, use an op-amp circuit that called an integrator, which generates a sawtooth waveform and is compared to a known reference voltage of opposite polarity wherein applied to the integrator. This is performed until the integrator to return zero at the output. The input voltage is a function of the reference voltage and the measured sawtooth waveform time period. The measurement of run-down time is made by a digital counter clocked with a square wave. This allows longer integration times that give higher resolutions [48] [49]. In Figure 3.7 a basic block diagram is shown.

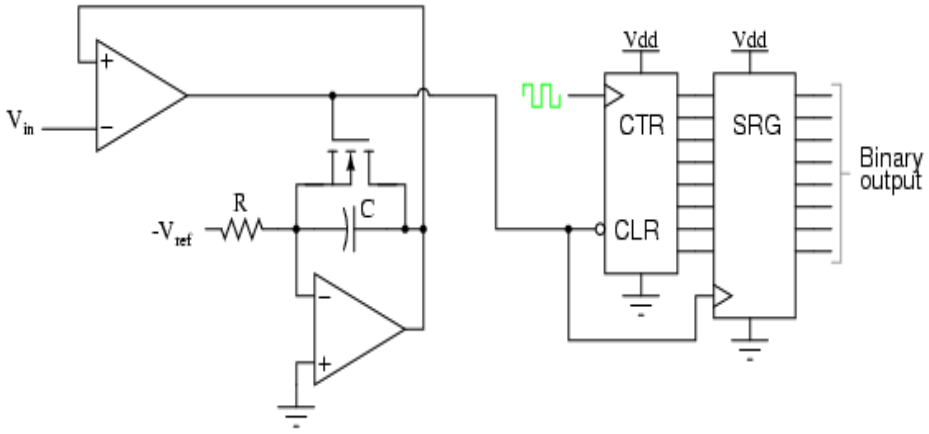

Figure 3.7 Dual Slope (integrating) ADC [49]

Firstly, a voltage input (unknown voltage) is applied to an integrator. Then a voltage reference Vref of opposite polarity is applied to the same integrator so as to perform the comparison between the two voltages. The reference voltage is applied to an IGBT capacitor-discharging transistor scheme, which is essentially a latching circuit clocked by the clock signal.

When the voltage input is bigger than the output of the comparator then the integrator charges the capacitor *C*, while the counter counts at a rate to be determined by the clock frequency. When the capacitor charged up to a voltage level equal to the input voltage V_{in}, then the output of the comparator goes high, loading the country's output into the shift register for a final output.

When the value of the integrator output voltage drops to zero, then the output of the comparator returns to a low state, clearing the counter and enables the integrator to ramp up the voltage again. When the integrator output voltage falls to zero, the comparator output switches back to a low state, clearing the counter and enabling the integrator to ramp up voltage again as indicated by the [49].

The Dual Slope converter can achieve high resolution but to do so at the expense of speed [48]. Also, it integrates the input voltage resulting in less noise. It has low latency and low power consumption.

3.6.5. Successive Approximation Register (SAR) ADC

One method of addressing the digital ramp ADCs shortcomings is the so-called successive-approximation ADC. The only change in this design is a very special counter circuit known as a successive-approximation register. Instead of counting up in a binary sequence, this register counts by trying all values of bits starting with the most significant bit and finishing with the least-significant bit. Throughout the counting process, the register monitors the comparator's output to see if the binary count is less than or greater than the analog signal input, adjusting the bit values accordingly. The way the register counts is identical to the "trial-and-fit" method of decimal-to-binary conversion, whereby different values of bits are tried from MSB to LSB to get a binary number that equals the original decimal number. The advantage to this counting strategy is much faster results: the DAC output converges on the analog signal input in much larger steps than with the 0-to-full count sequence of a regular counter.

Without showing the inner workings of the successive-approximation register (SAR), the circuit looks like this:

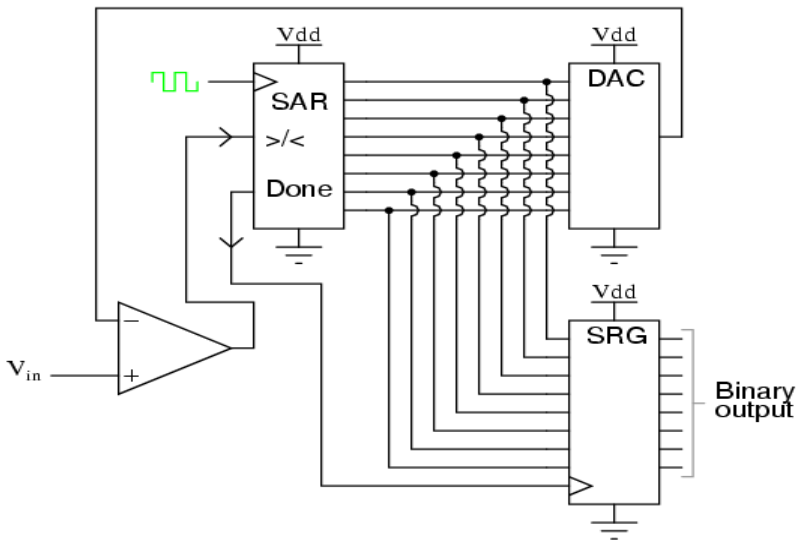

Figure 3.8 Successive Approximation Register (SAR) [47]

It should be noted that the SAR is generally capable of outputting the binary number in serial (one bit at a time) format, thus eliminating the need for a shift register. Plotted over time, the operation of a successive-approximation ADC looks like this [47].

The SAR converter is for applications that required good resolution and high accuracy in a satisfying speed. It features by zero cycle latency and low latency time. Provides low power consumption and it has an economic price.

3.7. Comparison of ADCs Architectures

Like the current sensor, the ADCs applies also cannot combine all features a satisfactory level. Table 2 shows the comparison of the ADC converters on the main levels.

Details/Sensors	HALL EFFECT		FLUXGATE SENSOR	SHUNT RESISTORS	MAGNETORESITIVE SENSOR		ROGOWSKI COIL	CURRENT TRANSFORMER
Measurement Current	AC/DC		AC/DC	AC/DC	AC/DC		AC	AC
Core	Yes/No		Yes	No	No		No	Yes
Current Sensor Type	Open Loop	Close Loop	Close loop	-	AMR	GMR	Close Loop	-
Accurasy	Low	Medium	High	High	Medium	High	Medium	Low
Bandwith	20kHz - 800kHz		<1 MHz	<1 MHz	>2MHz		>1MHz	<1MHz
Saturation and Hysteresis problem	Yes		Yes	No	No		No	Yes
Linearity	Low		Medium	High	Medium		High	Low
Isolation	Galvanic		Galvanic	-	Galvanic		Galvanic	Galvanic
Current Range	Medium		Medium	Low	Medium/High		High	Medium
Thermal Drift	Yes		Yes	Yes	Yes		No	Yes
Loss	Medium		Medium	High	Medium		Low	High
Size	Small		Small	Small	Small		Normal	Big
Cost	Cheap	Normal	Expensive	Cheap	Normal		Cheap	Normal

Table 2 Comparison of ADCs architectures

The architectures can be compared and someone to choose the appropriate one, depending on the application specification to be used.

The Delta Sigma, Integrating Dual Slope ADCs are suitable for high accuracy applications, but with moderate speeds. In contrast to Flash, which provides high speed up to 1 GMps to a satisfactory resolution up to 16 bit but with low accuracy.

The latency has to do with the modifications made to each converter. For this reason, as we see the SAR and Integrating Dual Slope ADCs feature a low latency, because to they are not needed so many conversions such as the Delta Sigma and Pipeline which presenting high latency of the input signal to output.

The Flash and Pipeline ADCs are offered for input signals with high bandwidth bigger than 1MHz in contrast to the rest which they have limited bandwidth in the input.

A factor in choosing the converter is the consumption. The consumption an inverter depends on several factors, such as speed, the internal conversion of signal and various components that accompany it. With these features, we find the Flash ADC. It has been inevitable to has not a high consumption with both high speeds.

The cost of converters differs.The SAR and Delta Sigma ADCs offers an economical solution for simpler applications. The FLASH and Pipeline ADCs for the most demanding applications are significantly more expensive.

4. Isolation Technologies

Often the measurement systems affected by external unwanted signals, such as voltage, current, temperature, flow measurements etc. as resulting in harming measurement systems and destroying measurement accuracy. To overcome these problems, the electronic measurement systems make use of electrical isolation. The use of electrical isolation as known galvanic isolation provides reliable measurements in adverse conditions [50].

In the galvanic isolation, there is not a direct electrical connection between the circuits. Its purpose is to separate electrical circuits and to limit the transient overvoltages. The galvanic isolation prevents any DC path [51] and non-acceptable stream flow [52].

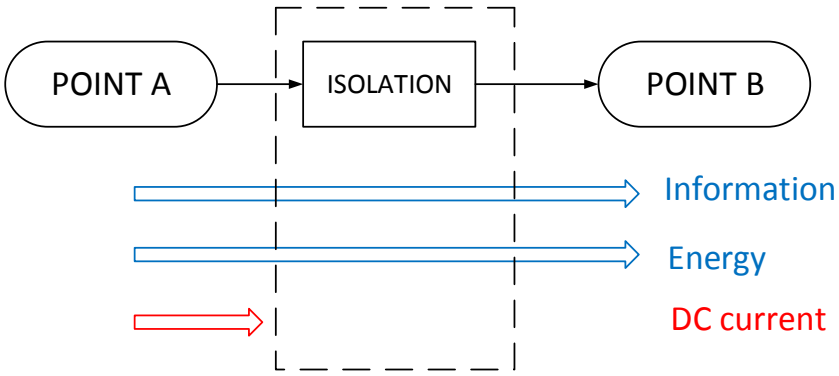

Figure 4.1 Isolation

In galvanic isolation offers separation of electrical circuits to eliminate unwanted signals on the PCB, which can be exposed to external factors. Provide protection for expensive equipment, to the data from transient voltages, to the elimination of group loop noise, confinement of electrical noise, increased common-mode voltage rejection, fault tolerance, ground potential differences to the user [50][53]. The desirable signals can pass between galvanically isolated circuits, contrary to stray currents or inductive currents which are blocked [54].

Considering the point of application which is required to make the isolation, the technics of the isolation differ. There are two forms of signal isolation, which are separated in analog isolation when the signal is still analog and the digital isolation when the signal is received processed from the ADC and it is in a digital form.

The galvanic isolation allows in the isolation circuits to communicate magnetic through a transformer, with light through an optoisolator [55] and with differential voltage through a capacitor [56].

4.1. Isolation Architectures

The main topologies of the isolation in a system are the inductive isolation, which exploits magnetic fields, the optocoupler which provides isolation by using light, a form of electromagnetic radiation and the capacitive isolation exploiting electric fields [57].

4.1.1. Optical Isolation

The optical isolators are based on the transmission of the signal using light by a LED and a photo-diode. The operation of it is based on a voltage applied across the LED and this in the continue produces a signal in the form of light. The signal is transmitted across the area of isolation and the photodiode receives light and converts it to its original form. There are also several other insulation techniques based on optical isolation which has different performances.

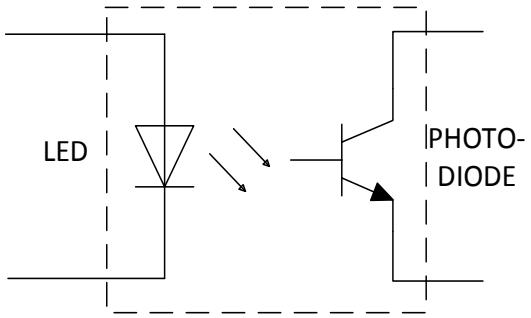

Figure 4.2 Optical Isolation

The optical isolation is one the most frequently used method, by providing a number of benefits in the isolation, such as shielding from electrical and magnetic noise, due that the signal transfer by light. Also, due to the existence of the LED and the photodiode, the technique becomes slower and the signal transmission is reduced, also results in high consumption and wear of components [50].

4.1.2. Capacitive Isolators

The isolation of the capacitor is less frequent isolation methods because this method is less robust than the other methods [56]. The capacitive isolation is based on an electric field that changes depending on the charge level to a coupling capacitor. This change is detected along an isolation barrier and is proportional to the level of transmission signal [50].

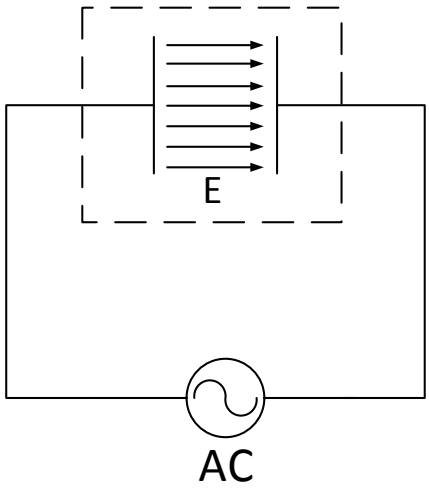

Figure 4.3 Capacitive Isolation

Like all methods, this method also has some advantages and disadvantages. The main advantage is that it is not affected by magnetic fields because of the signal transfer by use of an electric field. Due to the simplicity of the process makes a fast signal transfer technique. The disadvantage of this method is that it is prone to interference from external magnetic electric fields. In strong electric fields, there is the possibility of a change of signal [50].

4.1.3. Inductive Isolation

The inductive isolation exploiting the magnetic fields [57] created by the current flow in a coil induced in a second coil which located in a short distance. The induction is dependent on the current in the first coil. Essentially, the function described as the operating principle transformer [58]. This principle is called mutual induction and is the basis of the inductive isolation [50].

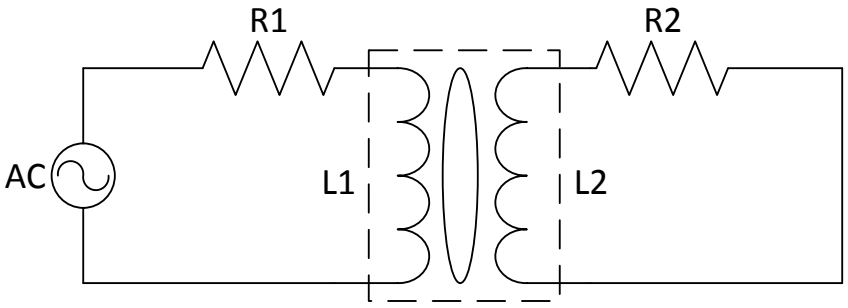

Figure 4.4 Inductive Coupling

In the inductive isolation, the two windings separated by an insulating layer that prevents any physical signal transmission. The signal is transmitted inductively due to the current changes flowing in the primary winding to the secondary winding causing the same current value (for conversion 1:1) along the insulating barrier. This technique provides high-speed transmission similar to the capacitive technique. The disadvantage of the inductance isolating is that the data transmission is performed using magnetic fields, so it is simultaneously susceptible to interference from the external magnetic field [50].

4.2. Separation of materials in a board

The galvanic isolation has the aim to isolate the power circuit and the isolation of signals.

The isolation of the circuit power supply is the most important part of the circuit operation, because the isolation in the input, isolates the two electrical provisions so that the none of electric route between them (infinite resistance) and bans the electromagnetic interferences in the circuit which are transferred from the mains or from some other source of power, protecting the circuit from external interference and increasing safety of the users of electronic device.

The components have the property of emitting electromagnetic signals. The fast transfers situations of the powers devices in combination with the parasitic devices generate electromagnetic noise, resulting in a bad designing to be affected the circuit. By isolating the circuit signals is achieved minimizing parasitics signals, which will lead in reducing losses and electromagnetic noise [59].

So it is easily perceived that it should take a number of improvements in the designing of the circuit of power electronics to reduced as much possible the electromagnetics interferences. As indicated in [57], to achieve a good isolation some designing standard should be followed.

4.3. Comparison of Isolation Technologies

The isolation techniques have significant differences between them. In the table 3 gathered the main differences and they are presented in detail.

Details/ Technologies	Optical Isolation	Capacitive Isolation	Inductive Isolation
Signal	Light	Differential Voltage	Magnetic Flux
Speed switching	Low	High	High
Immunity	High	Medium	Low
Power dissipation	Medium	Good	High
Power consumption	High	Medium	Medium
Longevity	Low	High	High

Table 3 Comparison of isolation technologies

What is observed in the above table is the difference in the signal transmission in each technique. In the case of optical isolation, the signal transferred by light, in the capacitive isolation with differential voltage and the inductive couplers with magnetic flux.

Both the optical isolation, because of the signal conversion process in light and the reverse process become slower. This technique during the transfer of data with light is armored from electrical and magnetic noise in comparison to the other two technologies which affected by external magnetic and electric fields.

The inductive isolation has the ability to transfer large energy flow. For this reason, the application is mainly in transformers.

The optical isolation, due to its complexity, has a higher energy consumption and damage to the components. The capacitive isolation and Inductive isolation, because of their simplicity of the construction are quite fast, without large consumption during the transfer of signals and with longer life.

5. Operation Amplifiers

The operation amplifier is a prefabricated monolithic circuit of small dimensions which behaves as a voltage amplifier, combined with other external components forming voltage amplifier, active filters etc. The operation amplifier has two inputs and one output. In the input supplied with U_P and U_N, such in the Figure 5.1. The U_N called inversion input and the U_P called non-inverting input [60][61].

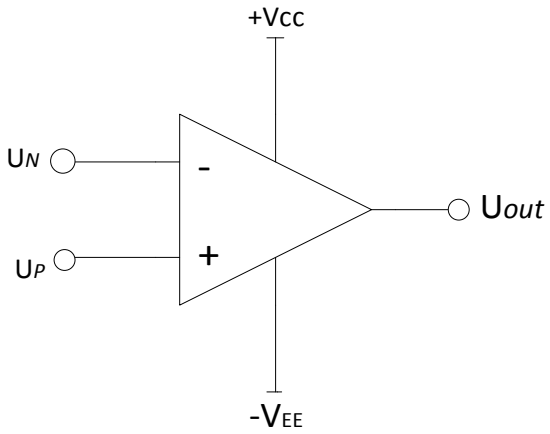

Figure 5.1 Operation Amplifier

The input voltage in the operation amplifier U_{in} is the difference:

$$U_{in} = U_P - U_N \tag{5.1}$$

The output voltage U_{out} is:

$$U_{out} = A\ U_{in} \tag{5.2}$$

Where *A* is the gain voltage of the operation amplifier.

An ideal operational amplifier has infinite voltage amplification, infinite input impedance, zero output impedance and a frequency range from 0 to infinity. In fact, these values are finite. The amplification is regulated by negative feedback which is provided with the appropriate connection between of resistors from the output to the inverting input.

This section will deal with the design and analysis of analog circuits, which contain the operational amplifier as a structural element. Therefore, it will be presented the function of the operational amplifier with useful models of operation.

5.1. Inverting Amplifier

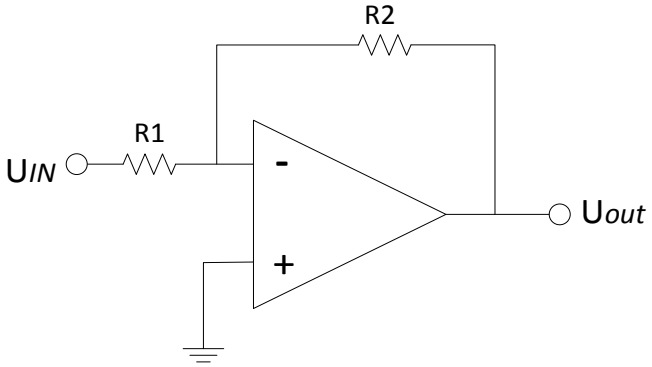

Figure 5.2 Inverting Amplifier

When connecting the voltage amplifier by inverting phase as shown in Figure 5.2, the input signal driven through the resistor *R1* to the inverting input. A part of the output signal is driven by negative feedback through the *R2* also to the inverting input. The non-inverting input connected to voltage 0. The voltage amplification (V_{out}) of amplifier is calculated by the following equation.

$$V_{out} = -\frac{R2}{R1} V_{in} \tag{5.3}$$

5.2. Non-Inverting Amplifier

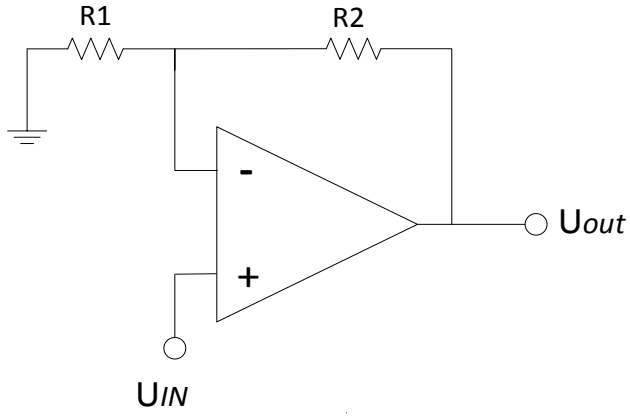

Figure 5.3 Non-Inverting Amplifier

When connecting the voltage amplifier without inverting phase as shown in Figure 5.3, the input signal driven into the non-inverting input. A part of the output signal is driven by negative

feedback through the voltage divider *R2-R1* to the inverting input. The voltage amplification (V_{out}) of amplifier is calculated by the following equation.

$$V_{out} = \frac{R1 + R2}{R1} V_{in} \tag{5.4}$$

5.3. Inverting Summing Amplifier

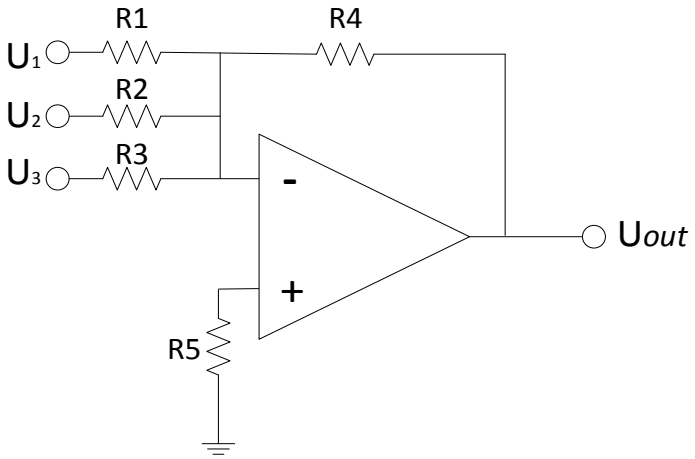

Figure 5.4 Inverting Summing Amplifier

The operational amplifier can be used in circuits summation voltages. As shown in Figure 5.4, the voltages *V1, V2* and *V3* summed, the value of the summed voltage depends on the resistances of *R1, R2* and *R3*.

The voltages *V1* to *V3* create a current through the resistors *R1* to *R3*. These currents are summed in the node of inverting input and then leaking through the *R4*, contributing to each one to the output voltage. The final output voltage can be calculated by summing up the individual output voltages arising by each input of the operational amplifier.

$$V_{out} = -R4\left(\frac{V_1}{R1} + \frac{V_2}{R2} + \frac{V_3}{R3}\right) \tag{5.5}$$

$$R5 = R1 \mathbin{/\!/} R2 \mathbin{/\!/} R3 \mathbin{/\!/} R4 \tag{5.6}$$

5.4. Difference Amplifier

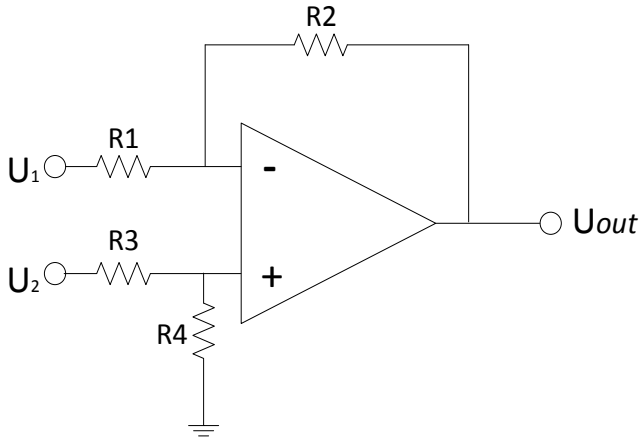

Figure 5.5 Difference Amplifier [61]

The operational amplifier can be used in circuits to remove voltages. As shown in the circuit in Figure 5.5, in the input applied the voltages *V1* and *V2* which through the resistors *R1* and *R3* creates a current. These currents are removed in the input of the operational amplifier and then a current flows through the *R2*, contributing to the output voltage. The value of voltage (V_{out}) of difference amplifier calculated by following equation.

$$V_{out} = \left(\frac{R1 + R2}{R3 + R4}\right)\frac{R4}{R1}V_2 - \frac{R2}{R1}V_1 \tag{5.7}$$

Where

$$R1 = R3 \; and \; R2 = R4 \tag{5.8}$$

$$V_{out} = \frac{R2}{R1}(V_{2-}V_1) \tag{5.9}$$

$$R1 \,/\!/\, R2 \;=\; R3 \,/\!/\, R4 \tag{5.10}$$

6. Combinations of Technologies

In this section, an approach for how we can combine the current sensors which were analyzed in Chapter 2 with the ADCs by Chapter 3 will be attempted. The criteria laid will be considered for the combinations and the comparisons are specifically. Concern mainly the between of them sequenced and coexistence on a PCB, the size of the application up to the cost.

All the sensors, of course, can be combined with all inverters because has not to do their combination with their internal architecture. All the architectures ADCs perform a comparison of an unknown input voltage with a known reference voltage [62].

6.1. The combinations of Sensors and ADCs

The Hall Effect sensor because of the simplicity of his construction, combined well with the equally simple construction circuit of the ADC SAR. The combination of those two is ideal for applications without great complexity in designing their circuits. The Hall Effect sensor is intended for applications not so much for high accuracy and this is what makes him fit appropriately with the ADC SAR. Also, their combination offers low operating consumption and low cost in their application.

The FluxGate sensor offers high resolution and high accuracy during his operation. It fits perfectly with the converter ADC Pipeline offered for equally fast applications high requirements. These two elements perform as well in high-frequency signals. Their combination is intended for high-potential applications in which there is not cost restriction.

The Shunt Resistors sensor hides specifics in the design, due to the absence of galvanic isolation. For this reason, when designing, it needs more attention than other sensors. As mentioned in paragraph 2.7, the problem of galvanic isolation is solved with the use of a particular converter AD 7403. This converter is Delta Sigma topology and solves the problem of isolation and relieve the designer from the complex design of the circuit. Equally, one can find many ready architectures with this combination, which the galvanic isolation provided in a separate circuit.

The Magnetoresistive is a sensor especially for applications that require high Bandwidth, for this mainly reason, match suitable with the converter SAR. Their combination offers very good accuracy in measurements with low energy consumption. Also, because of the small size, this combination can be used in applications with a restricted area of design. It is quite a satisfactory solution for high demanding applications and offers a low cost. Also, a very good combine with quite satisfying results can be done with the Pipeline ADCs and Delta Sigma ADC.

The Rogowski Coil is a generally flexible sensor that can design in various ways, so as to give a desired input signal to the each ADC. The features of this sensor combined quite well with the Integrating Dual-Slope ADC and SAR ADC. These converters because of the high Bandwidth which can perceive in the entry, is combined with very low consumption in the circuit, make this combination seem ideal.

The Current Transformer is mainly for bulky industrial applications without any particular limitation of space. Without high resolution and speed at which perceives the current can be combined quite well with most of its converters.

6.2. Summary of combinations

As mentioned above, all the ADCs operate with all sensors currents. Some combinations match more and some others less. Table 4 presents these combinations.

ADCs / Sensors	Hall Effect	Fluxgate	Shunt Resistors	Magnetoresistive Sensor	Rogowski Coil	Current Transformer
SAR	Good	Low	Medium	Good	Good	Good
Delta Sigma	Medium	Low	Good	Good	Medium	Medium
Flash	Medium	Medium	Low	Medium	Low	Medium
Pipeline	Low	Good	Low	Good	Medium	Low
Intergrating Dual Slope	Medium	Low	Medium	Medium	Good	Good

Table 4 Combination of Current Sensors with ADCs

6.3. The most prevalent combinations

Based on the needs of the application for which it is intended this thesis, resulting three predominant combinations. The combinations are 1. Shunt Resistor current sensor-Delta Sigma ADC, 2. Magnetoresistive current sensor-Pipeline ADC and 3. Rogowski Coil current sensor-Pipeline ADC, that in the continue explained the reasons.

6.3.1. Shunt Resistor- Delta Sigma ADC

With many advantages the shunt resistor as a current sensor, it is often the current sensor of choice for many systems. With the appropriate shunt resistor value, a variety of current ranges can be monitored.

The uses of this comparison show ideally for current sensing applications, where the voltage across a shunt resistor is monitored. The load current flowing through a shunt resistor, which produces a voltage at the input terminals of the Delta Sigma ADC. The analog input range is tailored to directly accommodate a voltage drop across of shunt resistor. The ADC provided isolation between the analog input from the current sensing resistor and the digital outputs.

The shunt resistors principles, used in combination with the ADC are determined by the requirements of each application, such as the terms of voltage, current, and power. Small values of resistors, minimize the power dissipation, whereas low inductance resistors avoid any induced voltage spikes and good tolerance devices reduce current variations.

Finally, taking into consideration the compromise between low power consumption and accuracy, it ranges at satisfactory levels for this application.

This combination offers excellent performance, even at low input signal levels, allowing to used shunt resistors with low value while maintaining system performance.

Ideal components for this application are shown to be the shunt resistors from ISABELLEHUTTE and from OHMITE in combination with one of two ADC from the Texas Instrument AD 7403 [26] and AMC1204- Q1 [63].

6.3.2. Magnetoresistive Sensor - Pipeline ADC

The Magnetoresistive Sensor is a sensor for specialized applications such as electrical motor control, DC/DC converter etc.

By detecting the current through two Wheatstone bridges and the ferromagnetic materials provides a high resolution for a much less field strength. With integrated signal conditioning amplifiers creates the desired voltage in the output of the sensor, so as to drives to the ADC. This facilitates greatly the design of the circuit.

The AMR sensors offer high bandwidth and with the right choice of ADC, the designer can play strengths with these sensors. A specialized company in the construction of AMR sensing elements is Sensitec GmbH, which for our application offers an ideal current sensor solution. The SMC3015 with 2MHz bandwidth, which in combined with a Pipelined ADC LTC 1420 of Linear Technology that delivers high-speed 10Msps and 12-bit resolution. For our application, the characteristics of the particular combination seen as an ideal solution.

Also one can find from specialized companies in the power electronics a lot of other solutions for this combination.

6.3.3. Rogowski Coil current sensor - Pipeline ADC

The Rogowski Coil with the property to measure a wide range currents without saturating seems as an ideal solution for many applications. The combination of this sensor with the Pipeline ADC seems as a good solution due to their features and the several options for applications that exist on the market.

The voltage generated at the edges of the Rogowski Coil is proportional to the rate of change of the AC current, which is driven through an integrator for processing the signal from the ADC. The signal is driven to the analog input range of Pipeline ADC

The ADC Pipeline that is currently available in the market, they have been designed specifically to support this kind of applications where there are high frequency input signals and requirement large dynamic range.Also, they are designed in a way that supports low voltage differential signaling in order to reduce the number of interface lines, thus allowing for high system integration density.

For the Rogowski Coil current sensors which have been designed and constructed for this work, the LTC 1420 ADC from Linear Technology and the ADC342x family from Texas Instrument are shown as ideal components.

7. Laboratory part

The design of the circuits and the measurement results are presented in this part. The measurements and the measurement results been made at the Fraunhofer IWES laboratory. The circuit was designed in Altium Design Software and measurements were taken from the following laboratory instruments WAYNE KERR PRECISION MAGNETIC ANALYZER model PMA3260A.

The key element that determined the choice of the sensors, is the frequency of the current (15A / 140kHz)which flowing through the system of wireless charging of vehicles. For the currents measuring were selected, a Magnetoresistive sensor (CMS3015), a Shunt Resistor sensor and a Fluxgate sensor (CASR15). Additionally, two different types of Rogowski coil sensors have been selected for design, the Planar Rogowski Coil (PRC) and the Combined Rogowski Coil (CRC) (Details are given in the Annex of the thesis).

7.1. Circuits design

In this part presented the schematic diagrams of circuits that have been designed in Altium Designer.

7.1.1. Schematic Circuits in Altium Design

Magnetoresistive current sensor

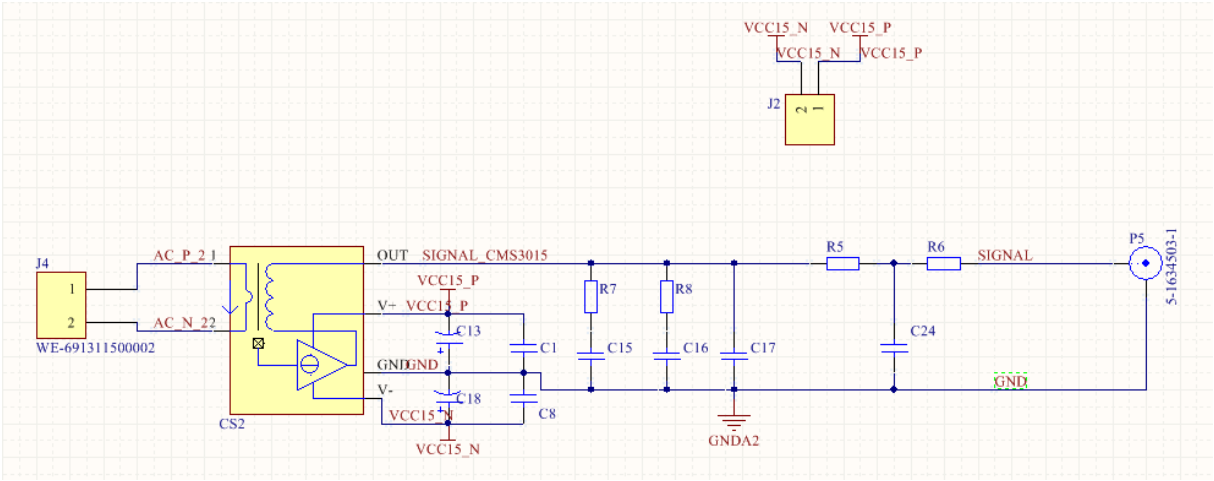

Figure 7.1 Schematic Circuits of Magnetoresistive current sensor

Shunt Resistor current sensor

As shown in Figure 7.2, it has been used an isolated delta-sigma modulator and an isolated power supply ADUM 5401.

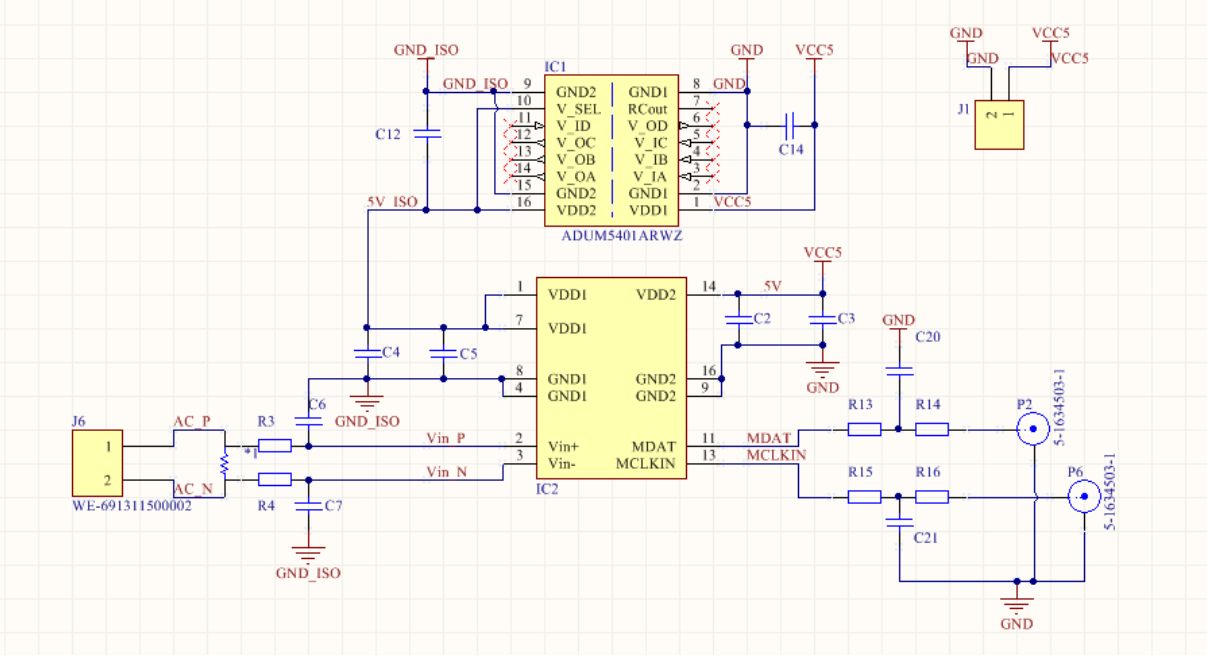

Figure 7.2 Schematic Circuits of Shunt Resistor current sensor

Fluxgate current sensor

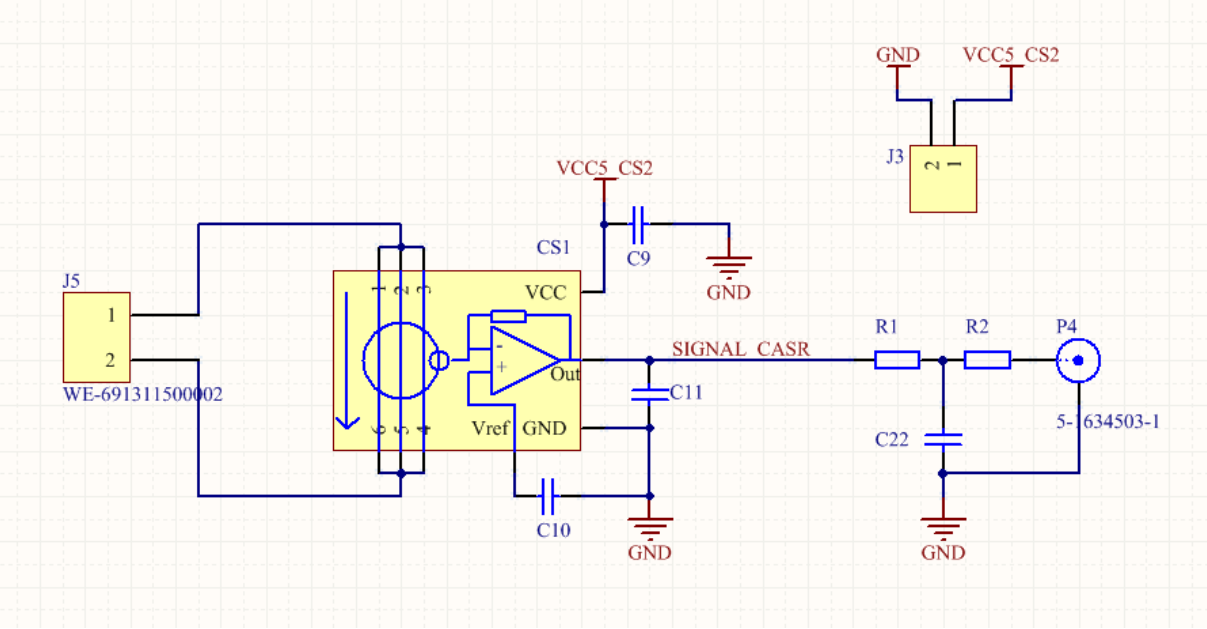

Figure 7.3 Schematic Circuits of Fluxgate current sensor

Planar Rogowski Coil current sensor (PRC)

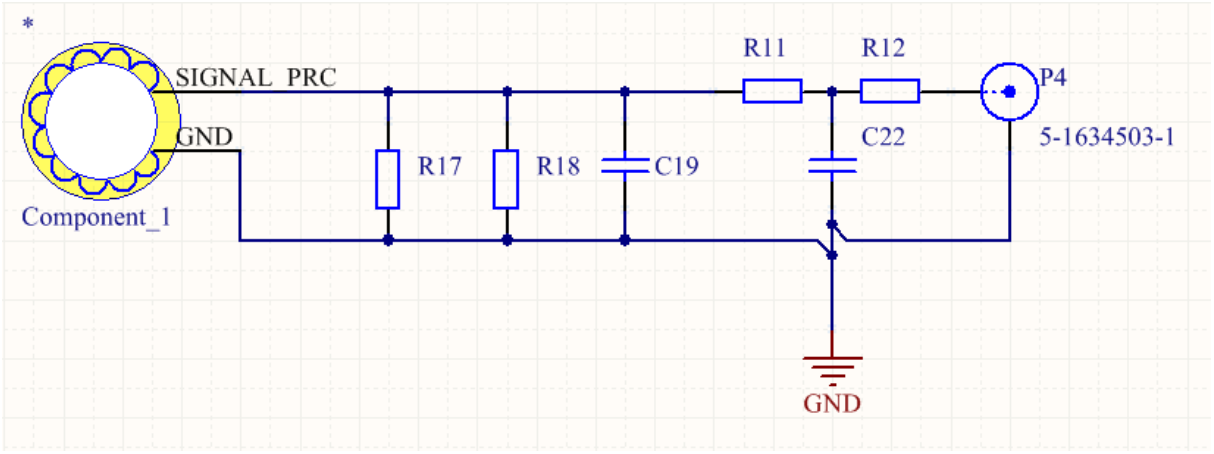

Figure 7.4 Schematic Circuits of Planar Rogowski Coil current sensor (PRC)

Combined Rogowski Coil current sensor (CRC)

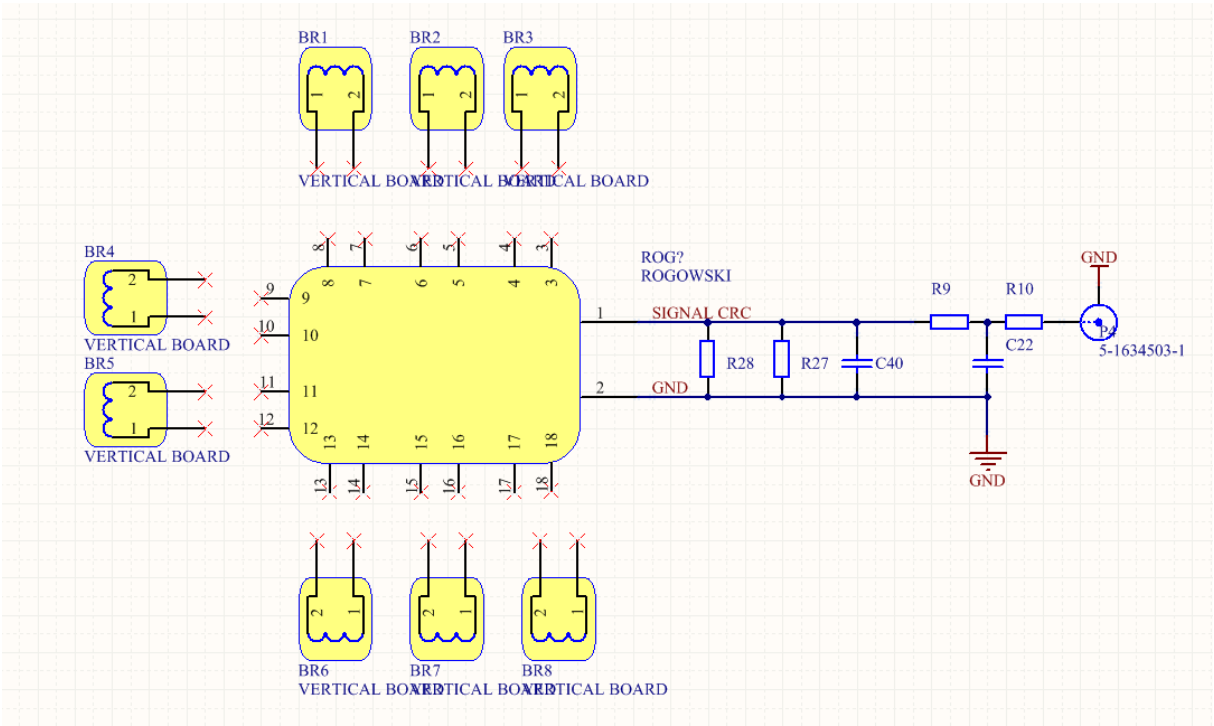

Figure 7.5 Schematic Circuits of Combined Rogowski Coil current sensor (PRC)

7.1.2. Printed Circuit Boards (PCB) design

Combined Rogowski Coil (CRC) current sensor

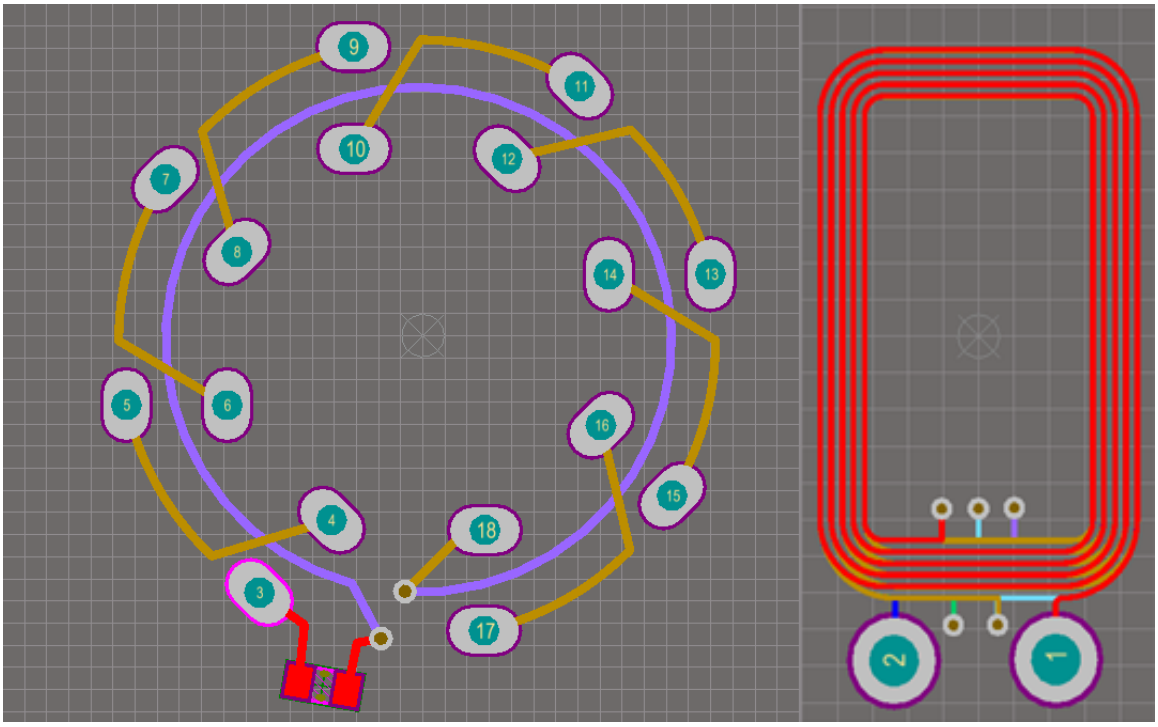

Figure 7.6 Left: Main board of Combined Rogowski coil, Right: Assistant board of Combined Rogowski coil

Planar Rogowski Coil (PRC) current sensor

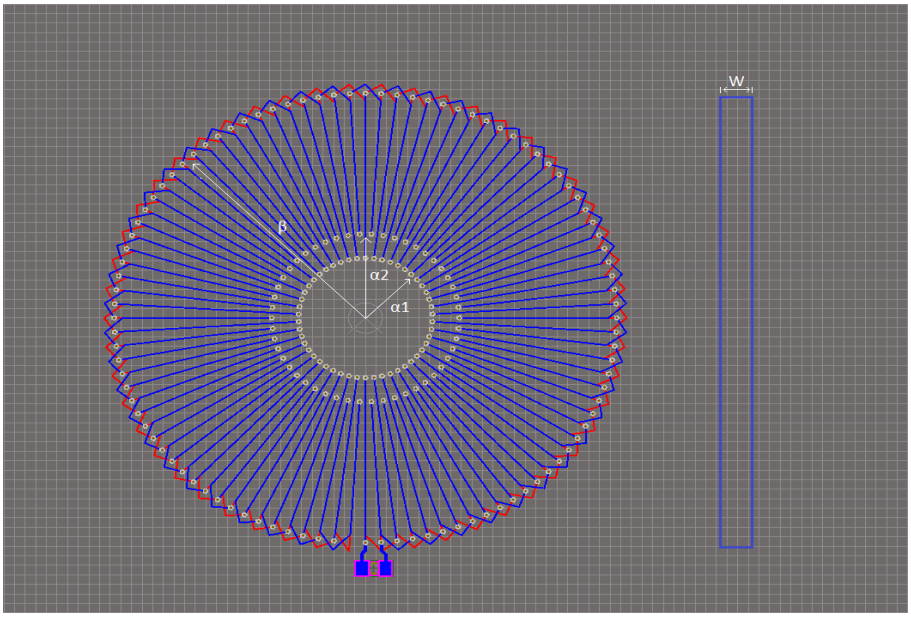

Figure 7.7 Circuit of PCB Planar Rogowski Coil PRC

Printed Circuit Board (PCB) design

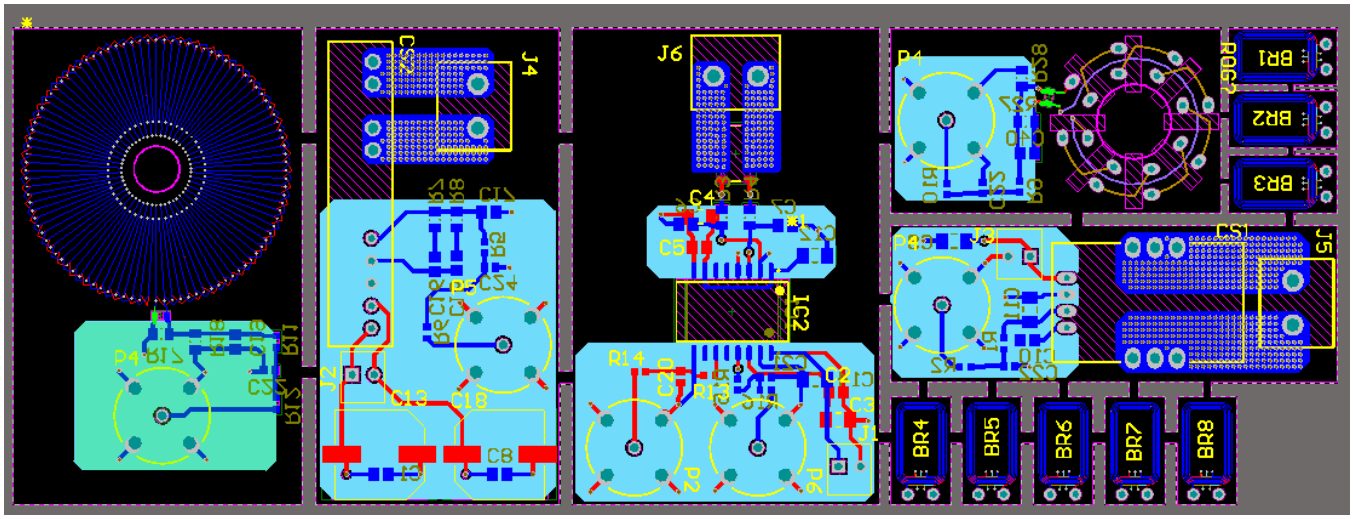

Figure 7.8 Printed Circuit Board (PCB) design

3D Top Layer of Printed Circuit Board (PCB)

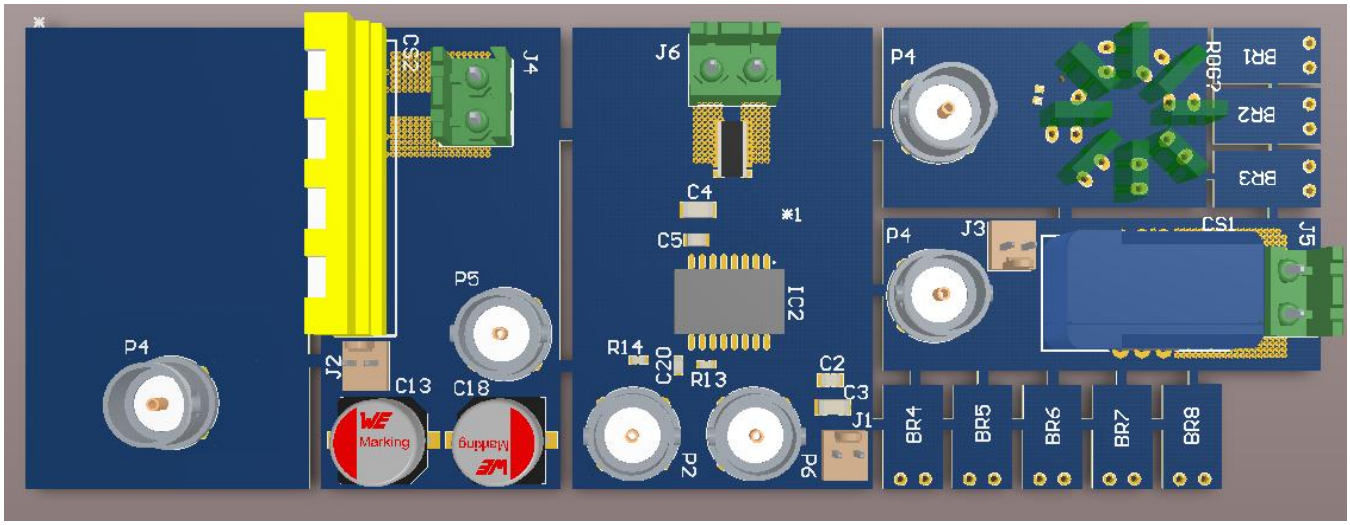

Figure 7.9 3D Top Layer of Printed Circuit Board (PCB) I

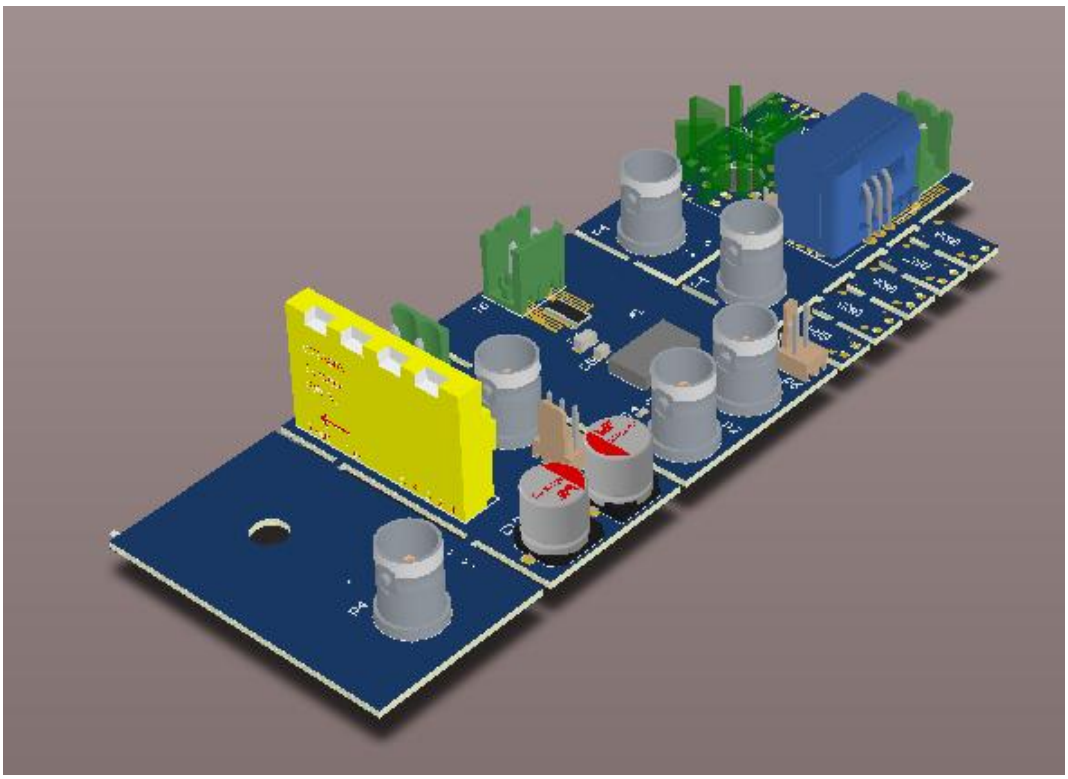

Figure 7.10 3D Top Layer of Printed Circuit Board (PCB)II

3D Bottom Layer of Printed Circuit Board (PCB)

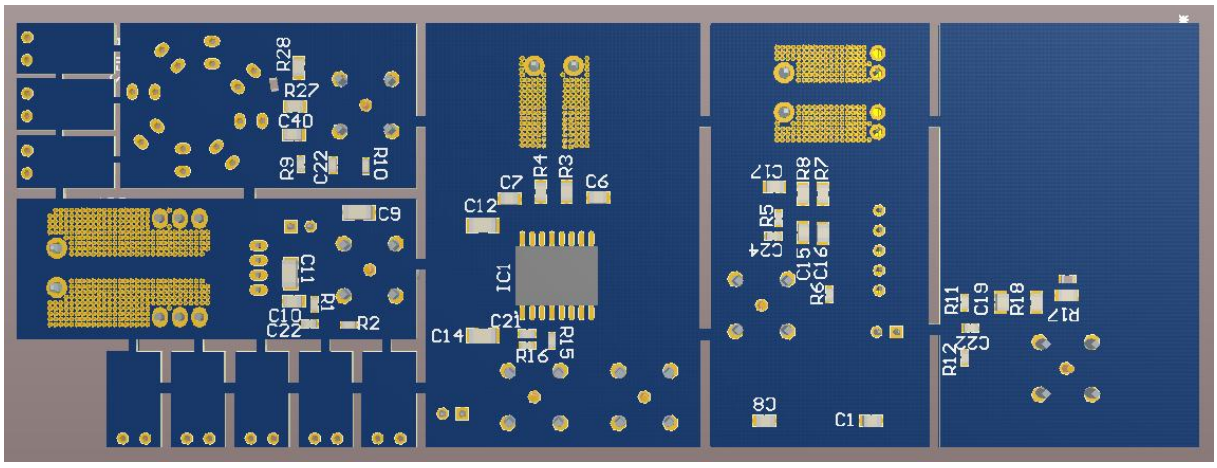

Figure 7.11 3D Bottom Layer of Printed Circuit Board (PCB)

7.1.3. The construction of printed circuit board (PCB)

At this part, we can see in Pictures 1 and 2, the printed board as it constructed.

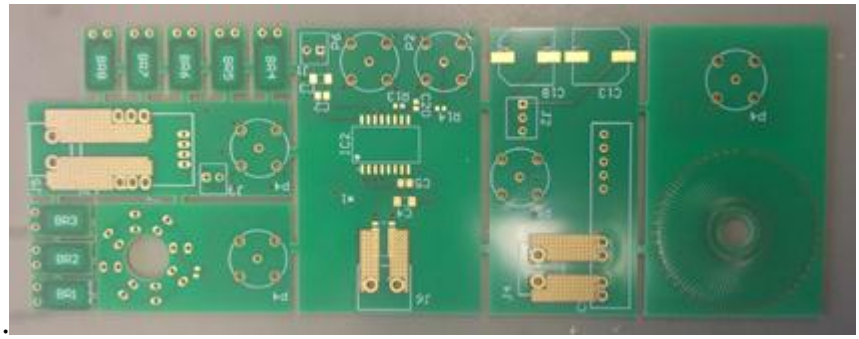

Picture 1 Top Layer of PCB

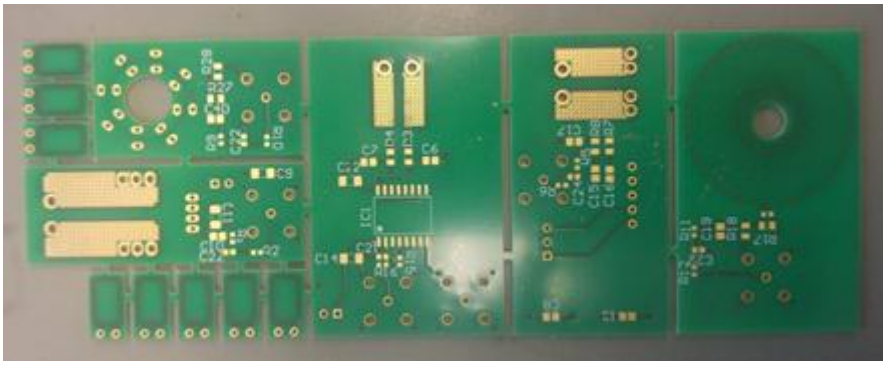

Picture 2 Bottom Layer of PCB

Subsequently, shown one by one the sensors as assembled in the laboratory.

Compined Rogowski Coil (CRC) current sensor

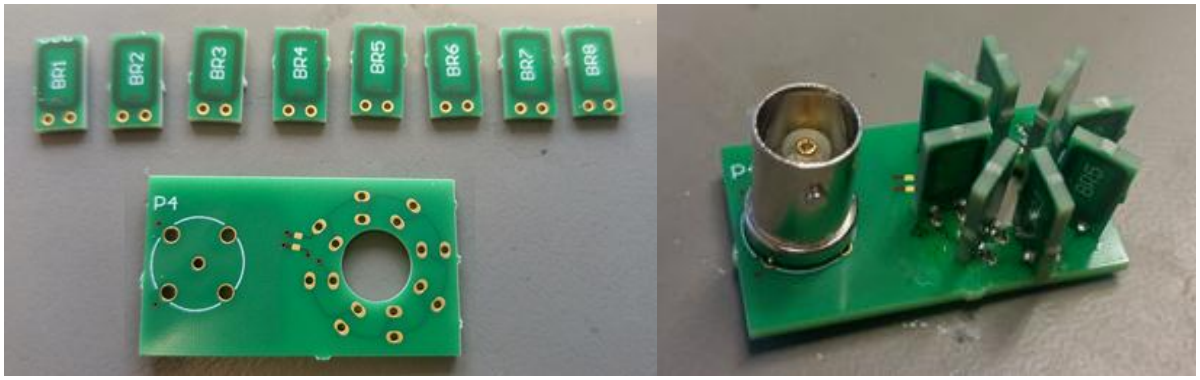

Picture 3 Combined Rogowski Coil (CRC) current sensor

Planar Rogowski Coil (PRC) current sensor

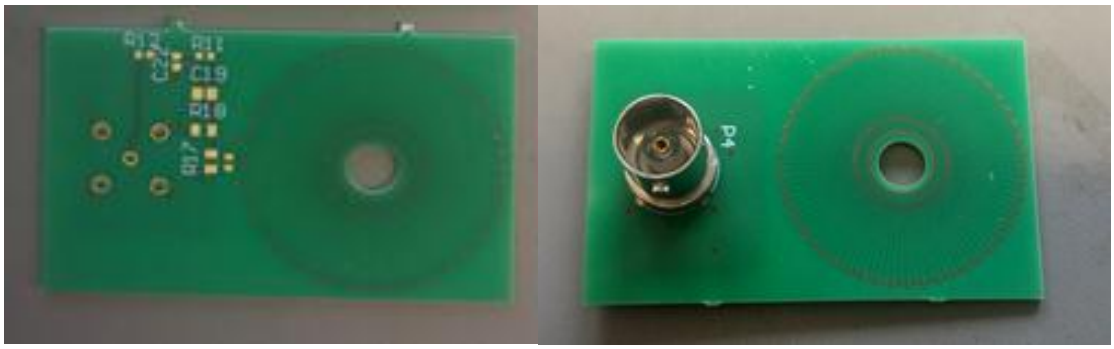

Picture 4 Planar Rogowski Coil (PRC) current sensor

Shunt Resistor current sensor

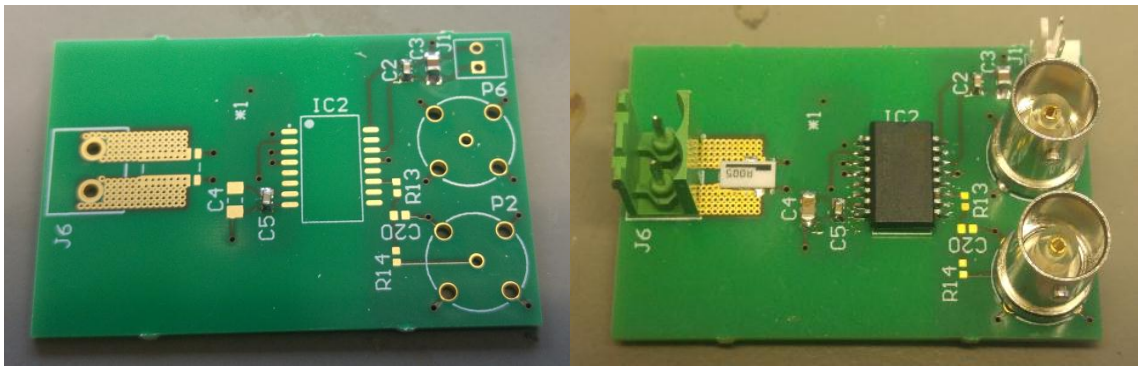

Picture 5 Shunt Resistor current sensor

Magnetoresistive current sensor

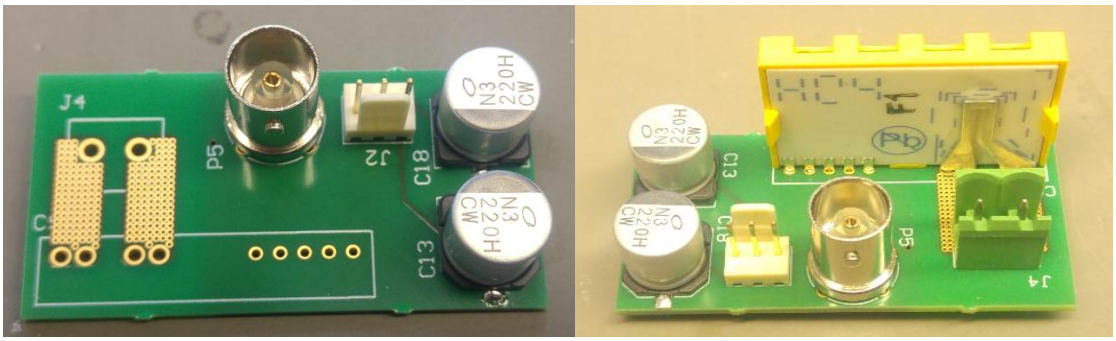

Picture 6 Magnetoresistive (Sensitec CMS3015) current sensor

Fluxgate current sensor

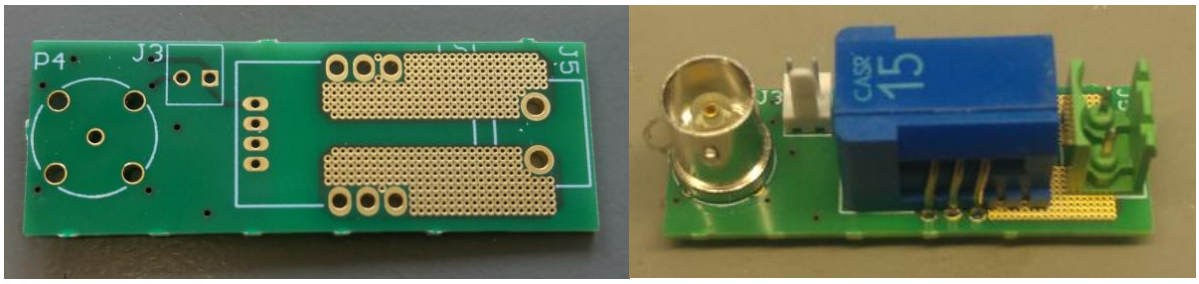

Picture 7 Fluxgate current sensor

And finally, we see their final form, as shown in Picture 8.

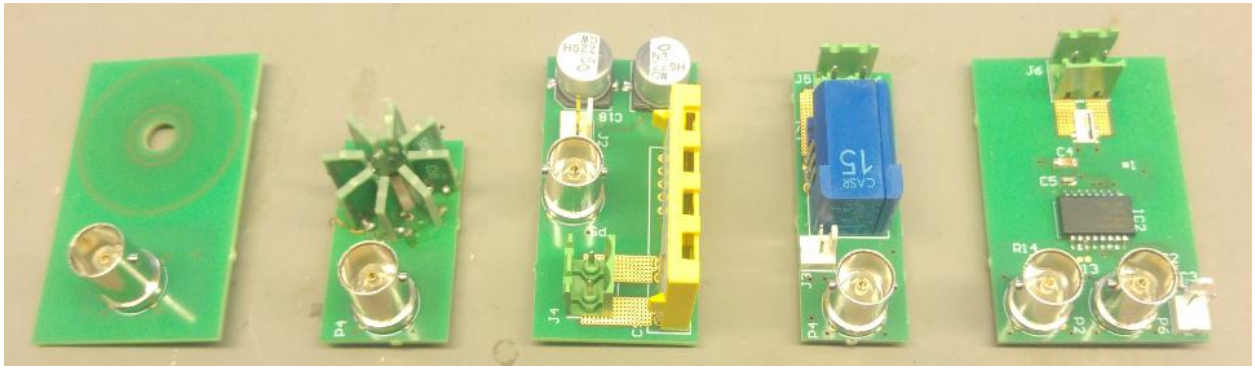

Picture 8 All the sensors

7.2. Laboratory Measurements

Measured results of electromagnetic parameters for the Rogowski Coils, by WAYNE KERR PRECISION MAGNETIC ANALYZER model PMA3260A

Picture 9

Measured results of electromagnetic parameters for the Rogowski Coils, by Agilent E7401A EMC ANALYZER 9kHz-1,5GHz

Picture 10

Planar Rogowski Coil

Freq. F	Self-induc. L	Internal-res. R	Impedance Z (Ω)	
5 kHz	3,85 µH	19,51 Ω	19,52∟0,36°	19,51+0,12i
10 kHz	3,84 µH	19,53 Ω	19,52∟0,70°	19,51+0,23i
20 kHz	3,84 µH	19,52 Ω	19,53∟1,42°	19,52+0,48i
30 kHz	3,84 µH	19,53 Ω	19,54∟2,21°	19,52+0,75i
50 kHz	3,84 µH	19,54 Ω	19,57∟3,52°	19,53+1,20i
100 kHz	3,84 µH	19,54 Ω	19,69∟7,02°	19,54+2,41i
200 kHz	3,83 µH	19,55 Ω	20,13∟13,84°	19,54+4,81i
500 kHz	3,83 µH	19,59 Ω	23,00∟31,58°	19,59+12,04i
1 MHz	3,83 µH	19,73 Ω	31,16∟50,70°	19,73+24,11i
2 MHz	3,85 µH	20,18 Ω	52,50∟67,40°	20,17+48,47i
3 MHz	3,89 µH	20,95 Ω	76,30∟74,00°	21,03+73,34i

Table 5 Electromagnetic parameters of the Planar Rogowski Coil

Combined Rogowski Coil

Freq. F	Self-induc. L	Internal-res. R	Impedance Z (Ω)	
5 kHz	83,70 µH	46,80 Ω	46,65∟3,24°	46,57+2,63i
10 kHz	83,70 µH	46,80 Ω	46,88∟6,44°	46,58+5,25i
20 kHz	83,68 µH	46,63 Ω	47,75∟12,72°	46,57+10,51i
30 kHz	83,68 µH	46,68 Ω	49,18∟18,72°	46,57+15,84i
50 kHz	83,69 µH	46,62 Ω	53,49∟29,44°	46,58+26,29i
100 kHz	83,68 µH	46,63 Ω	70,26∟48,44°	46,61+52,57i
200 kHz	83,69 µH	46,69 Ω	115,06∟66,06°	46,68+105,16i
500 kHz	83,74 µH	47,10 Ω	267,25∟79,84°	47,14+263,06i
1 MHz	84,04 µH	48,20 Ω	560,2∟84,80°	50,77+557,89i
2 MHz	85,25 µH	52,60 Ω	1072∟87,20°	52,36+1070,72i
3 MHz	87,50 µH	64,00 Ω	1650∟87,80°	63,34+1648,78i

Table 6 Electromagnetic parameters of the Combined Rogowski Coil

In Tables 5 and 6 shown the measured results of electromagnetic parameters for the two Rogowski Coils in frequency range 5 kHz up to 3 MHz

CONCLUSION

The Planar Rogowski Coil and the Combine Rogowski Coil that constructed on PCB, which the equations how to conclude their features are presented in the Annex. Both of the coils present a very good linearity in low and high current and low sensitivity of the shift of position conductor passing through the coil. They provide accurate current measurement sine wave. Even they can be used for instantaneous power measurement.

References

[1] Priyabrata Sahoo. “Seminar report on wireless electricity (Witricity)”; Available from: http://de.slideshare.net/ASHISHRAJ5/wireless-electricity-report.

[2] Wikipedia. "Wardenclyffe Tower"; Available from: https://en.wikipedia.org/wiki/Wardenclyffe_Tower.

[3] Yungtaek Jang and Milan M. Jovanovic. "A contactless electrical energy transmission system for portable telephone battery chargers"; IEEE 2000, p. 726–32.

[4] Wikipedia. "Power Electronics"; Available from: https://en.wikipedia.org/wiki/Power_electronics.

[5] Fani Liakou. "Galvanically Isolated Wide-Band Current Sensors". Thesis.

[6] Texas Instruments AK. "Six ways to sense current and how to decide which to use"; Available from: http://e2e.ti.com/blogs_/b/precisionhub/archive/2015/07/10/six-ways-to-sense-current-and-how-to-decide-which-to-use?keyMatch=methods%20rogowski%20for % 20current%20measurement&tisearch=Search-EN-Everything.

[7] Morris A.S. "Principles of Measurement and Instrumentation. Prentice Hall". New York; 1993.

[8] Tamura-Europe LTD. "Current Sensors"; Available from: http://www.tamura-europe.co.uk.

[9] Sensors and Actuators. "Sensors"; Available from: http://sensors-actuators-info.blogspot.de/2009/08/magnetoresistive-sensor.html.

[10] Νικόλαος Σπύρου. "Ηλεκτροτεχνικά Υλικά Ι"; Πάτρα, 2009.

[11] Honeywell. "Closed Loop Current Sensors"; Available from: http://sensing.honeywell.de/products/Current-Sensors/Closed-Loop/CSN/Ne/3025/N/3034.

[12] Powerguru. "Transducers Based on Fluxgate Technologies"; Available from: http://www.powerguru.org/transducers-based-on-fluxgate-technologies/.

[13] Electronic Tutorials. "The Current Transformer"; Available from: http://images.google.de/imgres?imgurl=http://www.electronics-tutorials.ws/transformer/.

[14] Ashaben Mehul Patel. "Current measurement in power electronic and motor drive applications". Thesis. University of Missouri-Rolla; 2007.

[15] David E. Shepard, Donald W. Yauch. "An Overview Of Rogowski Coil Current Sensing"; 2012.

[16] Sneha Lele. "Piezoelectric Transformer and Hall-Effect Based Sensing and Disturbance Monitoring Methodology for High-Voltage Power Supply Lines". Thesis. University of Western Ontario; 2013.

[17] Power Electronic Measurement (PEM). "Rogowski Coil"; Available from: http://www.pemuk.com/how-it-works.aspx.

[18] Wikipedia. "Rogowski coil"; Available from: https://en.wikipedia.org/wiki/Rogowski_coil.

[19] Pierre TURPIN. "A New Class of Rogowski Coil Split- Core Current Transducers"; Available from: http://www.powerguru.org/a-new-class-of-rogowski-coil-split-core-current-transducers/.

[20] Ljubomir A. Kojovic, Robert Buresh. Practical Aspects of Rogowski Coil Applications to Relaying 2010; IEEE PSRC.

[21] Resistorguide. "Shunt resistor"; Available from: http://www.resistorguide.com/shunt-resistor/.

[22] Intersil Americas LLC. "Sensing Elements for Current Measurements" 2014.

[23] Do-Yun Kim, Jung-Hyo Lee, Taeck-Kie Lee, Chung-Yuen Won. "Phase Current Sensing Method using Three Shunt Resistor for AC Motor Drive": In: IEEE Vehicle Power and Propulsion Conference; 2012, Seoul, Korea, p. 78–82.

[24] ISABELLEN HÜTTE. "Precision and power resistors"; Available from: http://www.isabellenhuette.de.

[25] Ibrahim A. Metwally. Performance Improvement of Slow-Wave Rogowski Coils for High Impulse Current Measurement. Volume 13; 2013, p. 538–47.

[26] Analog Devices I. "Data sheet AD7403: 16-Bit, Isolated Sigma-Delta Modulator".

[27] Dr. Rolf Slatter. "High Bandwidth Magnetoresistive Current Sensors Open up New Possibilities in Power Electronics"; Available from: http://www.powerguru.org/high-bandwidth-magnetoresistive-current-sensors-open-up-new-possibilities-in-power-electronics.

[28] Sensitec GmbH; Available from: http://www.sensitec.com.

[29] McGuire T, Potter R. "Anisotropic magnetoresistance in ferromagnetic 3d alloys". Volume 11; 1975, p. 1018–38.

[30] Sensitec GmbH. "Magnetic Micro and Nanotechnology for Robust Sensor Solutions".

[31] Texas Instruments. "Principles of Data Acquisition and Conversion" 2015.

[32] Ραφαήλ Ψιάκης. "Αλγόριθμοι και υλοποίηση «mixed signal» κυκλώματος ανίχνευσης παλμών (Read-Out) υψηλής ταχύτητας". Διπλωματική Εργασία. Πανεπιστήμιο Πατρών; Ιούνιος 2015.

[33] Κωνσταντίνος Βασιλακόπουλος. "Μελέτη και Σχεδίαση Μετατροπέων Σήματος (D/A Converters)". Διπλωματική Εργασία. Πανεπιστήμιο Πατρών; 2013.

[34] Joao C., Vital Pedro, M. Figueiro. "Offset Reduction Techniques in High-Speed Analog to Digital Converters. Analysis, Design and tradeoffs, Analog Circuits and Signal Processing Series ed.". Springer Science and Business 2009.

[35] Βάσσω Χρησούλα. "Τεχνική απαλοιφής του offset σε υψηλής ταχύτητας μετατροπείς αναλογικού σήματος σε ψηφιακό αρχιτεκτονικής Flash". Διπλωματική Εργασία. Αριστοτέλειο Πανεπιστήμιο Θεσσαλονίκης; Οκτώβριος, 2011.

[36] Walt Kester, Dan Sheingold, James Bryant. "The Data Conversion Handbook: Chapter 2, Fundamentals of sampled data systems". Newnes; 2005.

[37] Herbert Taub-Donald L.Schilling. "Principles of Communication System", 3rd ed.: McGraw-Hill Inc; 1987.

[38] Gabriel Torres. "How Analog-to-Digital Converter (ADC) Works: How It Works: Resolution"; Available from: http://www.hardwaresecrets.com/how-analog-to-digital-converter-adc-works/3/.

[39] Maxim Integrated. "ADC and DAC Glossary: Tutorial 641" 2002.

[40] Νικόλαος Καραβίτης. "Μελέτη δομών μετατροπέων αναλογικού σήματος σε ψηφιακό". Διπλωματική Εργασία. Πολυτεχνείο Πατρών; 2008.

[41] All About Circuits. "Flash ADC: Chapter 13-Digital-Analog Conversion"; Available from: http://www.allaboutcircuits.com/textbook/digital/chpt-13/flash-adc/.

[42] Jim LeClare, Principal Member of Technical Staff. "A Simple ADC Comparison Matrix: Tutorial 2094". Maxim Integrated 2003.

[43] Figueiredo M, Goes J, Evans G. "General Overview of Pipeline Analog-to-Digital Converters", p. 5–45.

[44] Γεώργιος Αλέξανδρος Σίσκος. "Σχεδιασμός και Υλοποίηση ενός Μετατροπέα Αναλογικού Σήματος σε Ψηφιακό, τύπου Σίγμα Δέλτα, βασισμένου σε καινοτόμο Φίλτρο Αντιστάθμισης με χρήση FPGA". Διπλωματική Εργασία. Πολυτεχνείο Κρήτης, Χανιά; 2009.

[45] Walt Kester. "Which ADC Architecture Is Right for Your Application" 2005.

[46] Κωνσταντίνος Τσιάτουρας. "Μελέτη μετατροπέων ψηφιακού σήματος σε αναλογικό με την τεχνική Σιγμα Δελτα". Πάτρα; 2007.

[47] All About Circuits. "Delta-Sigma ADC: Chapter 13-Digital-Analog Conversion"; Available from: http://www.allaboutcircuits.com/textbook/digital/chpt-13/delta-sigma-adc/.

[48] Wikipedia. "Integrating ADC"; Available from: https://en.wikipedia.org/wiki/Integrating_ADC.

[49] All About Circuits. "Slope integrating ADC: Chapter 13 - Digital-Analog Conversion"; Available from: http://www.allaboutcircuits.com/textbook/digital/chpt-13/slope-integrating-adc/.

[50] National Instrument. "Isolation Technologies for Reliable Industrial Measurements"; Available from: http://sine.ni.com/np/app/main/p/ap/daq/lang/en/pg/1/sn/n17:daq,n21:41/fmid/2871/#toc0.

[51] Measurement Computing. "Noise Reduction and Isolation"; Available from: www.mccdaq.com.

[52] Wikipedia. "Capacitive Coupling"; Available from: https://en.wikipedia.org/wiki/Capacitive_coupling.

[53] Baoxing Chen. "Galvanic Isolation for Power Supply Applications": PELS Webinar.

[54] Maxim Integrated. "Glossary definition for galvanic isolation: Glossary Term: Galvanic Isolation"; Available from: https://www.maximintegrated.com/en/glossary/definitions.mvp/term/Galvanic%20Isolation/gpk/516.

[55] David Lohbeck. "Safety isolation protects users and electronic instruments: Understanding safety isolation rules and testing requirements enables you to address potential safety isolation vulnerabilities". National Instruments 2004.

[56] Michael Stock. "Galvanic Isolation: Purpose and Methodologies: Capacitors"; Available from: http://www.allaboutcircuits.com/technical-articles/galvanic-isolation-Purpose-and-Methodologies/.

[57] Analog Devices. "Analog Isolation Amplifiers: MT-071 Tutorial" 2009.

[58] Marie Christiano. "Transformer Isolation"; Available from: http://www.allaboutcircuits.com/technical-articles/transformer-isolation/.

[59] Πατσουράκης Νικόλαος. "Τεχνικές Συσκευασίας για Μετατροπείς Ισχύος". Athens; 2015.

[60] Πορλίδας Δημήτριος. "Τελεστικοί ενισχυτές: Κυκλώματα, Πειραματικές μετρήσεις και Μεθόδοι"; 2009.

[61] National Semiconductor Corporation. "Application Note 31 Operation Amplifier Circuits Collection" 2002.

[62] Maxim Integrated. "Design Considerations for a Low-Cost Sensor and A/D Interface: Application Note 3775"; Available from: https://www.maximintegrated.com/en/app-notes/index.mvp/id/3775.

[63] Texas Instruments. "Data Sheet AMC 1204-Q1: 20 MHz Second-Order Isolated Delta-Sigma Modulator for Current-Shunt Measurement" 2012–2013.

[64] Wikipedia. "Faraday's law of induction"; Available from: https://en.wikipedia.org/wiki/Faraday's_law_of_induction.

[65] Luka Ferković DI. Dependence of mutual inductance of a precise Rogowski coil on the primary conductor position. Zagreb, Croatia.

[66] Chiampi M, Crotti G, Morando A. "Evaluation of Flexible Rogowski Coil Performances in Power Frequency Applications". IEEE Transactions on Instrumentation and Measurement 2011;60(3):854–62.

[67] R. O. De Alessandro, M. D. Vélez Ibarra. "Design of a Current Measurement System in a Plasma Thruster with Rogowski Coil" 2013;11(1):119–125.

[68] G. Robles, J. M. Martinez, J. Sanz, B. Tellini, C. Zappacosta, M. Rojas. "Designing and tuning an air-cored current transformer for partial discharges pulses measurements". IEEE Instrumentation and Measurement 2008.

[69] Esmaeil Hemmati, S. Mohammad Shahrtash. "Evaluation of Unshielded Rogowski Coil for Measuring Partial Discharge Signals". IEEE 2012.

[70] Yi Wang, Jiaman Li, Yulan Hu, Ranran An, Zexiang Cai, Ruiwen He. "Analysis on the Transfer Characteristics of Rogowski-coil Current Transformer and Its Influence on Protective Relaying" 2013;05(04):1324–9.

[71] T. Guillod, D. Gerber, J. Biela, A. Musing. "Design of a PCB Rogowski Coil based on the PEEC Method": IEEE; 2012.

[72] D. G. Pellinen, M. S. Di Capua, E. Sampayan, H. Gerbracht and M Wang. "Rogowski coil for measuring fast high-level pulsed currents". Volume 11; 1980.

[73] W.F. Ray CH. "Rogowski transducers for measuring large magnitude short duration pulses". Savoy Place, London WC2R OBL, UK., IEE; 2000.

[74] W.F. Ray CH. "High-Performance Rogowski Current Transducers"; 2000, p. 3083–90.

[75] Chen Qing, Li Hong-bin, Zhang Ming-ming, Liu Yan-bin. "Design and Characteristics of Two Rogowski Coils Based on Printed Circuit Board". Volume 55, p. 939–43.

Annex

Designing PCB Rogowski coil

Preferred the design of the Rogowski coil current sensor because of the many featured in relation with the other sensors, as these are is the high linearity of the wide range of current measurement without magnetic saturation.

The Rogowski coils where are commercially available have limited bandwidth to some kHz, for this reason, preferred the design so that the bandwidth to be improved in MHz.

Rogowski Coil Magnetic Calculations

At the case of Rogowski Coil calculation, the function of it is based on Faraday's Law on induction, who mentioned that the induced electromotive force EMF in a circuit is equaled to the opposite of the rate of change of the passing magnetic flux from the circuit. If there is a coil with *N* turns and the flow which passes through each winding is altered with rate $\Delta\Phi/\Delta_t$, then the induced electromotive force EMF given by the relationship [64]:

$$E = -N\frac{\Delta\Phi}{\Delta t} \tag{8.1}$$

The above relationship give us the average value of EMF in a time interval Δ_t.

As shown in several publications such as [65] [66], the basic equation which can calculate the voltage *V* at the ends of the windings of the Rogowski Coil sensor is:

$$V = -M\frac{di}{dt} \tag{8.2}$$

This equation shows that the voltage that was developed across the coil is equal to the derivative of the current flowing through a conductor that crosses the air-core, multiplied by the mutual inductance. This is because when in a coil, passing a current which carried from a conductor, then a magnetic field is generated inside this.

To calculate the mutual inductance *M [H],* should first to consider the magnetic field *B,* from the bellow equation:

$$B = \frac{\mu_0\, I}{2\,\pi\, w} \tag{8.3}$$

Where *B [T]* is the magnetic field created, the μ_0 *[H/m]* vacuum magnetic permeability, *I [A]* is the current that flows through the conductor and $2\,\pi\, w$ *[m]* is the along of the winding.

Then, from the equation of the magnetic flux, calculated the φ *[WB]*

$$\varphi = \int B\, ds \tag{8.4}$$

where ds a small part of the surface.

$$\varphi = \frac{\mu_0\, I}{2\pi} w \int \frac{1}{x} dx = \frac{\mu_0\, I\, w}{2\pi} \ln\left(\frac{b}{\alpha}\right) \tag{8.5}$$

Where b the radius of the outside circle and α the radius of the internal circle.

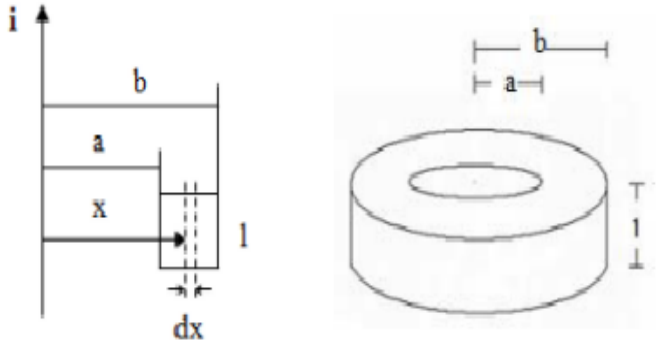

Figure A. 1 Rogowski coil [67]

Finally, replacing in the equation of magnetic flux φ, the values of construction from the sensor and multiply with the number of turns N, then the total value of the magnetic flux φ_c calculate by the bellow equation:

$$\varphi_c = \frac{\mu_0\, I\, w\, N}{2\,\pi} \ln\left(\frac{b}{\alpha}\right) \tag{8.6}$$

And the mutual inductance *M [H]:*

$$M = \frac{\varphi_c}{I} = \frac{\mu_0\, w\, N}{2\,\pi} \ln\left(\frac{b}{\alpha}\right) \tag{8.7}$$

The mutual inductance depends on the geometry of the coils, from the relative position of the conductor and the material in the area of provision of coils, *1H=1Wb/A* [67].

The self-inductance *L* is a measure of the amount of magnetic flux which produced for the current that flows in the coil [68] and is given by the by the equation [69] as:

$$L = \frac{\mu_0 N^2 h}{2\pi} ln\left(\frac{b}{\alpha}\right) \tag{8.8}$$

Equivalent circuit

The equivalent circuit of a Rogowski coil is shown in Figure A.2. It has a small mutual inductance *M*, owing to the air-core [70] which can be considered such as a voltage source $U_1(s)$ representing the full voltage caused by the current to be measured [71], in series to the inductance L0 and the self-resistance *R* of the coil. The R_m load resistance is very large [70] [72] and its will define the peration of the coil [25].

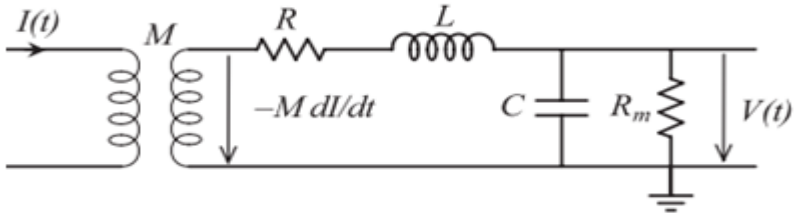

Figure A. 2 Electrical circuit of Rogowski Coil [25]

From the equivalent circuit of Figure A.2, the transfer function is given by the following equation:

$$H_1(s) = \frac{U_1(s)}{I(s)} = \frac{M\,s}{L\,C\,s^2 + \left(\frac{L}{R_m} + R\,C\right)s + \left(\frac{R}{R_m} + 1\right)} \tag{8.9}$$

Due to the very low value of the circuit resistance *R* in most cases ignored. So the simplified relation is the bellow:

$$H_1(s) = \frac{M\,s}{L\,C\,s^2 + \frac{L}{R_m}\,s + 1} \tag{8.10}$$

The transfer function shows that the voltage $U_1(s)$ is proportional to the *di/dt*, because the coil is only counts the *di/dt* [71].

Calculate the Bandwidth

To calculate the bandwidth will take us into consideration the following circuit in Figure A.3, which have been added additional elements of the of the signal cable to the load. As shown, have added the *Cc* which is the signal cable capacitance, *Rt* is the coil termination resistance, and *Rm* is the signal cable resistance.

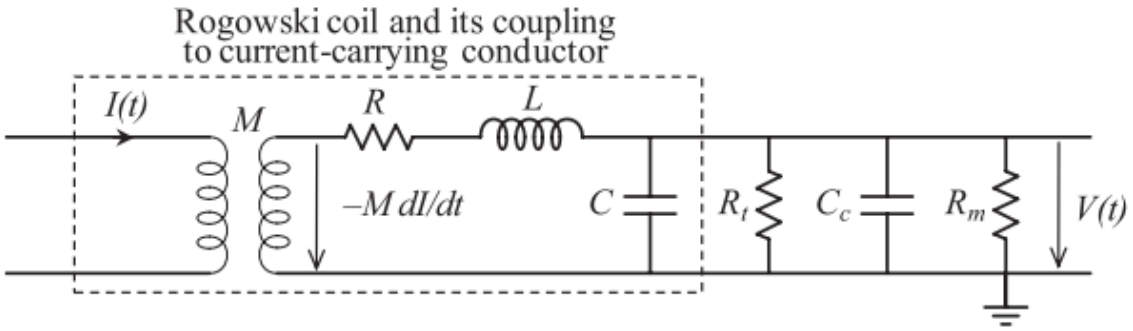

Figure A. 3 The electric circuit of Rogowski coil including the elements required in the design and calculation of bandwidth [25]

In an ideal circuit, the output voltage of the coil depends linearly on the frequency, but because of the engagement of the elements *R*, *L*, and *C*, this dependence is more complex, resulting in the terminal resistance *Rt* of the coil to appear a frequency characteristic with a plateau between the low *fl* and high *fh* angle frequencies [25].

Down of the frequency *fl* the gain of the coil decreases, as more than an upper limit frequency *fh* the gain again decreases, due to the inherent time delays of the coil and the integrator [73] [74]. From Figure A.3 we take the following equations for the lower and upper of "cutoff" frequencies in a −3 dB line.

Low Frequency:

$$R_1 = \frac{R_t R_m}{R_t + R_m} \tag{8.11}$$

$$f_l = \frac{R + R_1}{2\pi(L + R\,R_1\,C_1)} \cong \frac{R + R_1}{2\pi\,L} \tag{8.12}$$

High Frequency:

$$C_1 = C + C_c \tag{8.13}$$

$$f_h = \frac{L + R\,R_1\,C_1}{2\pi\,R_1\,L\,C_1} \cong \frac{1}{2\pi\,R_1\,C_1} \tag{8.14}$$

The Bandwidth defined as:

$$BW = f_h - f_l = \frac{1}{2\pi\,R_1\,C_1} - \frac{R + R_1}{2\pi\,L} \tag{8.15}$$

Circuit of Planar Rogowski Coil

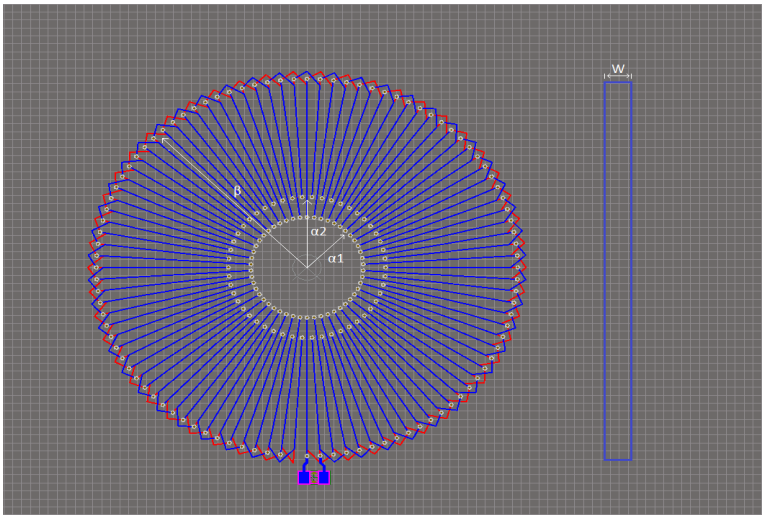

Figure A. 4 PCB of Planar Rogowski Coil (PRC)

In Figure A.4 shows the information which required for the calculations. The values used in the construction of the coil are the following:

TABLE I. Parameters of the coil.

Coil parameter	Specification
Outer radius, b	15,6 *mm*
Internal radius, a_1	3,8 *mm*
Inner radius of the compensation coil, α_2	5 *mm*
Thickness, h	2,4 *mm*
Number of turns, N	50
Width , W_{cu}	0,1 *mm*
High , h_{cu}	0.035 *mm*
Magnetic constant, μ_0	$1{,}256\ 10^{-6} H/M$
Copper resistivity,ρ_{cu}	$1{,}68\ 10^{-8} \Omega\ m$

TABLE II. Calculated parameters of the coil.

Model Parameter	Specification
Mutual Inductance, *M*	0,061 μH
Self-resistance, *R*	16,493 Ω
Self-inductance, *L*	3,06 *mH*
Self-capacitance, *C*	13,64 *pF*
The coil termination resistance, R_t	10 Ω
The signal cable capacitance, C_c	10 *nF*
The signal cable resistance, R_m	52 Ω
Rogowski Voltage, *V*	0,808 *V*
Low frequency, f_l	894,759 *kHz*
High frequency, f_h	2,754 *MHz*
Bandwidth, *BW*	1,864 *MHz*

Calculations

Mutual Inductance:

$$M = \frac{\mu_0 N h}{2\pi} ln\left(\frac{b}{a_1}\right) + \frac{\mu_0 N h}{2\pi} ln\left(\frac{b}{\alpha_2}\right) = 6{,}12\ 10^{-8} H \tag{8.16}$$

Current:

$$\frac{d}{dt} i(t) = 1{,}319\ 10^{7} A/s \tag{8.17}$$

The output voltage of Rogowski Coil:

$$V = M * \frac{di}{dt} = 0{,}808\ V \tag{8.18}$$

Self-Inductance:

$$L = \frac{\mu_0\ N^2\ h}{2\ \pi}\ ln\left(\frac{b}{a_1}\right) + \frac{\mu_0\ N^2\ h}{2\ \pi}\ ln\left(\frac{b}{a_1}\right) = 3{,}06\ 10^{-6} H \tag{8.19}$$

Self-Resistance:

$$R = \frac{\rho_{cu}\ L_{wire}}{W_{cu}\ h_{cu}} = 16{,}493\ \Omega \tag{8.20}$$

Self-Capacitance:

$$Ro = \frac{D_{ext} + D_{int}}{2} = 19{,}4\ mm \tag{8.21}$$

$$r = \frac{D_{ext} - D_{int}}{2} = 0{,}012\ mm \tag{8.22}$$

$$C = \frac{4\ \pi^2\ \varepsilon_0\ \ Ro}{ln\left(\frac{Ro}{r}\right)} = 13{,}64\ pF \tag{8.23}$$

Low frequency:

$$R1 = \frac{Rt\ \ Rm}{Rt + Rm} =\ 8{,}38\ Ohm \tag{8.24}$$

$$fl = \frac{R + R1}{2\ \pi\ (L + R\ \ R1\ \ C1)} = 890{,}759\ kHz \tag{8.25}$$

High Frequency:

$$C1 = C + Cc =\ 10{,}014\ nF \tag{8.26}$$

$$fh = \frac{L + R\ \ R1\ \ C1}{2\ \ \pi\ \ R1\ \ L\ \ C1)} = 2{,}754\ MHz \tag{8.27}$$

Bandwidth:

$$BW = fh - fl = 1{,}864\ MHz \tag{8.28}$$

Combined Rogowski Coil CRC-Theoretical

For the Combined Rogowski Coil As shown in Figure A.5 required to design, a main PCB and eight auxiliary PCB which satisfy the particular application. In the main PCB circuit, there is the series circuit to feed the assistant boards, which produce the induced voltage [75].

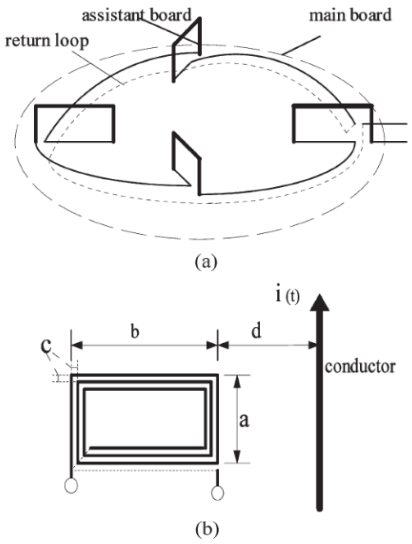

Figure A. 5 (a) Construction of main board of CRC. (b) Assistant board and conductor of CRC [75]

TABLE III. Parameters of the coil.

Coil parameter	Specification
Width of assistant board, a	12 mm
Length of assistant board, b	4,9 mm
Distance between the wires, c	0,2 mm
The distance from the conductor, d	2,8 mm
Number of $assistant\ boards$, N	8
Turns of loops on one assistant board, k	30
Magnetic constant, μ_0	$1{,}256\ 10^{-6} H/M$

TABLE IV. Calculated parameters of the coil.

Model Parameter	Specification
Mutual Inductance, *M*	0,222 μH
Self-resistance, *R*	45,8 Ω
Self-inductance, *L*	77,361 μH
Self-capacitance, *C*	83,086 *pF*
The coil termination resistance, R_t	10 Ω
The signal cable capacitance, C_c	10 *nF*
The signal cable resistance, R_m	52 Ω
Rogowski Voltage, *V*	1,238 *V*
Low frequency, f_l	100,191 *kHz*
High frequency, f_h	1,973 *MHz*
Bandwidth, *BW*	1.872 *MHz*

The mutual inductance of a CRC is given by:

$$M' = \sum_{i=1}^{k} \int_{d+(i-1)\,c}^{d+b+(i-1)\,c} \frac{\mu_0 * (a - 2 * (i-1) * c)}{2 * \pi * x}\, dx = 0{,}028\ \mu H \tag{8.29}$$

$$M = N * M' = 0{,}222\ \mu H \tag{8.30}$$

Current:

$$\frac{d}{dt} i(t) = 1{,}319\ 10^7\ \frac{A}{s} \tag{8.31}$$

The output voltage of Rogowski Coil:

$$V = M * \frac{d}{dt} i(t) = 2{,}925\ V \tag{8.32}$$

Self-inductance:

$$L = \frac{\mu_0 * (k * N)^2 * a}{2 * \pi}\ ln\left(\frac{b}{d}\right) = 77{,}361 \mu H \tag{8.33}$$

Self-Resistance:

$$R = \frac{\rho_{cu} * L_{wire}}{W_{cu} * h_{cu}} = 45{,}8\ \Omega \tag{8.34}$$

Self-Capacitance:

$$C = \frac{2 * \pi * \varepsilon_0 * l_{wire}}{ln\left(\frac{2 * rs}{d}\right)} = 83{,}086\ pF \tag{8.35}$$

Low frequency:

$$R1 = \frac{Rt * Rm}{Rt + Rm} = 8{,}38\ Ohm \tag{8.36}$$

$$fl = \frac{R + R1}{2 * \pi * (L + R * R1 * C1)} = 100{,}191\ kHz \tag{8.37}$$

High Frequency:

$$C1 = C + Cc = 10{,}083\ nF \tag{8.38}$$

$$fh = \frac{L + R * R1 * C1}{2 * \pi * R1 * L * C1)} = 1{,}973\ MHz \tag{8.39}$$

Bandwidth:

$$BW = fh - fl = 1{,}872\ MHz \tag{8.40}$$